

1999-10-12

# Verification and Adaptation of an Infiltration Model for Water at Various Isothermal Temperature Conditions

Joseph F. Schaffer  
*Worcester Polytechnic Institute*

Follow this and additional works at: <https://digitalcommons.wpi.edu/etd-theses>

---

## Repository Citation

Schaffer, Joseph F., "Verification and Adaptation of an Infiltration Model for Water at Various Isothermal Temperature Conditions" (1999). *Masters Theses (All Theses, All Years)*. 1061.  
<https://digitalcommons.wpi.edu/etd-theses/1061>

This thesis is brought to you for free and open access by Digital WPI. It has been accepted for inclusion in Masters Theses (All Theses, All Years) by an authorized administrator of Digital WPI. For more information, please contact [wpi-etd@wpi.edu](mailto:wpi-etd@wpi.edu).

Verification and Adaptation of an Infiltration Model for Water at Various Isothermal  
Temperature Conditions

by

Joseph F. Schaffer

A Thesis

Submitted to the Faculty

of the

WORCESTER POLYTECHNIC INSTITUTE

in partial fulfillment of the requirements for the

Degree of Master of Science

in Civil Engineering

August 1997

Approved:

Dr. Cindy Sue-Shih Kao, Major Advisor

Dr. Frederick L. Hart, Head of Department

## ***TABLE OF CONTENTS***

Abstract . . . . .	iii
Acknowledgments . . . . .	iv
Chapter 1: Introduction . . . . .	1
1.1: Scope . . . . .	1
1.2: Applicability . . . . .	1
1.3: Overview . . . . .	2
Chapter 2: Background . . . . .	4
2.1: Darcy's Law . . . . .	4
2.2: Darcy-Buckingham Law . . . . .	5
2.3: Richard's Equation . . . . .	6
2.4: Permeability . . . . .	6
2.5: Capillarity . . . . .	7
2.6: Plug Flow . . . . .	10
2.7: Green and Ampt . . . . .	12
2.8: Poiseuille's Law . . . . .	13
2.9: Kao and Hunt . . . . .	14
2.10: Temperature Effects on the Kao and Hunt Model . . . . .	15
2.10.1: Viscosity . . . . .	16
2.10.2: Surface Tension . . . . .	17
2.10.3: Other Effects . . . . .	18
2.10.4: What Parameters should Not Change with Temperature . . . . .	21
2.10.5: Sensitivity . . . . .	22

Chapter 3: Experiment	23
3.1: Experimental Variation	23
3.2: Experimental Apparatus	24
3.2.1: Whole System	24
3.2.2: Zero Pressure Head Reservoir	26
3.2.3: Soil Column, Caps, and Thermocouples	26
3.2.4: Vacuum Chamber	29
3.2.5: CN76000 Temperature Controller and Associated Hardware	30
3.2.6: Heater	30
3.2.7: Chiller	32
3.2.8: Fluid Pumps	33
3.2.9: Data Acquisition Computer	34
3.3: Experimental Procedures	34
3.3.1: Sample Preparation	35
3.3.1a: <i>Packing</i>	35
3.3.1b: <i>Plugging with machine screws</i>	36
3.3.1c: <i>Continuity test for leaks</i>	37
3.3.1d: <i>End Preparation</i>	37
3.3.1e: <i>Permeability Test</i>	38
3.3.1f: <i>Cleaning</i>	38
3.3.2: Setting up the Experiment	39
3.3.3: Initiation of the Experiment	40
3.3.4: Environmental Control	41
3.4: Technical Problems with Using Vacuum	41
3.5: Conclusion	42
Chapter 4: Presentation of Data	43
4.1: All Data	43
4.2: Refined Data	47
4.3: Conclusion	51
Chapter 5: Discussion	52
5.1: Difference Between the Model and the Data	52
5.2: Causes of Experimental Error	53
5.2.1: Human Factors	54
5.2.2: Non-Zero Pressure Head	55
5.2.3: Temperature Normalization of Imbibed Water	55
5.3: Data-Model Error	57
5.3.1: Temperature vs. Error	57
5.3.2: Distance vs. Time <sup>0.5</sup> Slopes	58
5.4: Conclusion	59
Appendix: Permeability Testing with Air	61
References	63

***ABSTRACT***

A series of one dimensional horizontal infiltration experiments were performed to investigate the predictive capabilities of the Kao and Hunt model. By modifying pristine laboratory apparatus, a reasonable range of soil temperatures was achieved. Experiments were run at approximately 5 °C, 20 °C, and 35 °C. Distilled water was used as an infiltrating liquid and silica powder was used as soil. The infiltrating liquid was dispensed into the column at zero pressure head. The results of the experiments show that the model is adaptable to a range of temperature conditions by modifying terms for the liquid effects of the model, viscosity and surface tension. Experimental data and model predictions differed by 30 percent at most. Although the change in the rate of infiltration across the range of temperatures is perceivable, it is small in comparison to the effects caused by heterogeneity encountered in nature.

## ***ACKNOWLEDGMENTS***

This project may not have been possible without the help of these people:

- Dr. Cindy S. Kao for her effort and support throughout this project
- Dr. Frederick L. Hart and Dr. Paul P. Mathisen for their guidance
- Dr. Robert A. D'Andrea for his patience with me
- Arthur Bealand for his craftsmanship, patience, and time
- Joe for his friendly advice
- My Parents for their love and support

## **1: INTRODUCTION**

This chapter will cover:

- scope
- applicability
- overview

The scope will describe what this project seeks to accomplish in general. Applicability will review the fields that can benefit from infiltration studies. The overview will quickly cover some of the major points of the paper to give an overview.

### **1.1: SCOPE**

This project deals with the infiltration of water into soil under different isothermal temperature conditions. It used a previously derived model to estimate infiltration, and these estimates were compared with laboratory results. The model was changed slightly to adapt to different temperatures. This project was limited to the validation and adaptation of a model for the horizontal infiltration of water into dry soil under zero pressure head. In this project, the effects of temperature were tested, and the model was adapted to match the changes in temperature.

### **1.2: APPLICABILITY**

Urban areas are unlike naturally occurring terrain because of buried structures. Some buried structures can introduce heat into the ground. These structures include:

- underground power and telecommunication conduits
- steam transmission lines
- sewer and water pipes
- underground building space
- pavement cover

Buried conduits and building spaces may be heated. Sewer pipes will tend to be warm from wash water. Pavement cover tends to be hotter than natural terrain due to the dark color and the lack of plant cover on most roadways. The important point to note with all of these applications is that if contaminant transport is affected by the temperature, then these buried appurtenances will have a localized affect on transport.

Consider a contaminant that will move faster in warmer soils. If a plume of said contaminant hits a steam pipe, the contaminant may tend to travel parallel to the hot pipe. This situation may be aggravated by the type of backfill used. For instance, a highly permeable soil like sand would allow a good deal of flow.

### **1.3: OVERVIEW**

This thesis paper consists of:

- background material
- experimental procedures and apparatus
- presentation of data
- discussion of data

The background material deals with the theoretical development of the model used in this study in addition to other relevant theoretical points. The basic laws and



concepts are introduced, and the previously derived model is then presented. The modification of the model for temperature is then explained.

The section describing experimental procedures and apparatus reviews the fully developed experiments. Procedures are outlined in detail to document the experiment and aid in reproducibility of the experiments. The lab equipment is described in words and photographs to show the nature of the lab work.

The final sections show and discuss the data. The presentation of data presents the data in a compact and reasonable form. This section also describes the refinement of the data collected. The discussion section reviews the results of the experiments and draws conclusions from the results.

## **2: BACKGROUND**

In this review of background material, the development of the Kao and Hunt Model will be described. The following concepts and laws can be used to best describe the development of this model.:

- Darcy's Law
- Darcy-Buckingham Law
- Richard's Equation
- Permeability
- Capillary
- Plug Flow

The Green and Ampt Model will also be described briefly. Some other basic properties and laws will also be described.

Nomenclature will be introduced as needed with the equations and not repeated throughout the paper. Unless specific quantities are presented, the units used are F(force), L(length), T(time), M(mass).

### **2.1: DARCY'S LAW**

Darcy developed an equation describing the flow of water through soil that forms the backbone of hydrologic science as known today:

$$v = -K \frac{\partial H}{\partial z} \quad [2-1]$$

where:  $v$  = specific discharge (L/T)  
 $K$  = saturated hydraulic conductivity(L/T)  
 $H$  = hydraulic head(L)  
 $z$  = length(L)

(Das 132, Fetter 145)

Specific discharge is the flow rate per unit area through the sample. The saturated hydraulic conductivity is the constant of proportionality relating flowrate to the head gradient and it reflects the ability of the soil to conduct flow. Hydraulic head is the sum of pressure head and elevation head. This equation is the basis of many other soil relations and has been verified countless times by many subsequent researchers.

## **2.2: DARCY-BUCKINGHAM LAW**

Darcy's Law deals exclusively with saturated water flow. Darcy's Law was later modified by Buckingham for unsaturated flow to produce the Darcy-Buckingham flux law:

$$v = -K(h) \frac{\partial H}{\partial z} \quad [2-2]$$

where  $K(h)$  = hydraulic conductivity as a function of pressure head(L/T)

The pressure head is negative in partially saturated systems, indicating that the soil water is under tension and so it will be referred to as suction head when addressing pressure head in the unsaturated zone. It is a function of soil moisture content; with decreasing moisture content,  $h$  becomes more negative. Equation 2-2 takes into account the variability of the hydraulic conductivity with initial moisture content.

### 2.3: RICHARD'S EQUATION

If a mass balance is solved for a soil system based on the Darcy-Buckingham Law, the resulting differential equation is Richard's Equation:

$$\frac{\partial \Theta}{\partial t} = \frac{\partial}{\partial z} \left( K(h) \frac{\partial h}{\partial \Theta} \frac{\partial \Theta}{\partial z} \right) - \frac{\partial K(h)}{\partial z} \quad [2-3]$$

where:  $\Theta$  = moisture content  
 $t$  = time

Richard's Equation is a powerful tool in modeling infiltration; however, it requires that the parameters  $K(h)$  and  $h(\Theta)$  must be field measured. These parameters are non-linear, which makes measurements and calculations cumbersome.

Richard's Equation, although theoretically rigorous, may not be accurate. Since Richard's Equation relies on field measured parameters, the error in measuring these parameters is introduced into the equation.

### 2.4: PERMEABILITY

Permeability is a value describing the geometry of the soil matrix and is related to hydraulic conductivity by the following relation:

$$K = \frac{\rho g k}{\mu} \quad [2-4]$$

where:  $K$  = saturated hydraulic conductivity

$\rho$  = liquid density  $\left( \frac{F}{L^3} \right)$

$g$  = acceleration of gravity  $\left(\frac{L}{T^2}\right)$

$k$  = permeability ( $L^2$ )

$\mu$  = liquid dynamic viscosity  $\left(\frac{FT}{L^2}\right)$

A soil with a higher permeability will tend to restrict the flow of water less than a soil of low permeability. Permeability for naturally occurring soils can differ by orders of magnitude.

## 2.5: CAPILLARITY

The variation in  $h$  and  $K$  in the unsaturated zone can be explained in terms of capillarity. The basic concepts of capillarity are described first.

The difference in pressure between the inside and the outside of a liquid film bubble can be described by the equation:

$$\Delta P = \frac{2\sigma}{r} \quad [2-5]$$

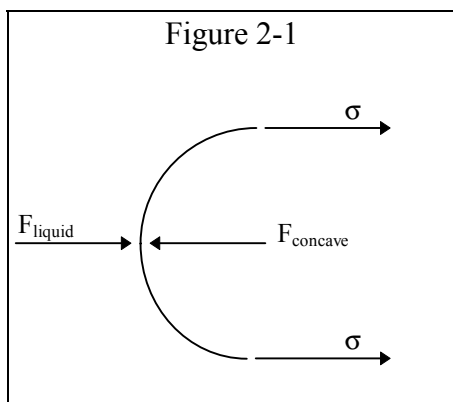
where:  $\Delta P$  = pressure differential  $\left(\frac{F}{L^2}\right)$  = capillary pressure

$\sigma$  = interfacial tension  $\left(\frac{F}{L}\right)$

$r$  = bubble radius (L)

(Adamson, 4-52)

It can be seen that the smaller the radius of the bubble, the higher the pressure inside of the bubble. The forces within this system can be arranged as shown in Figure 2-1.

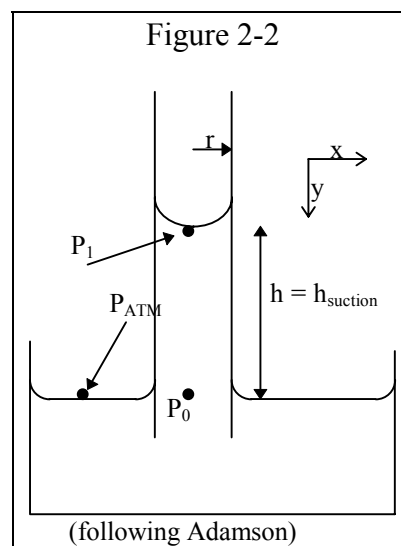


It follows that the force on the concave side of the meniscus,  $F_{\text{concave}}$ , is higher than the force on the convex side of the meniscus,  $F_{\text{liquid}}$ . Consequently, the pressure on the concave side of the meniscus is higher than the pressure on the convex side of the meniscus. The interfacial tension is the result of

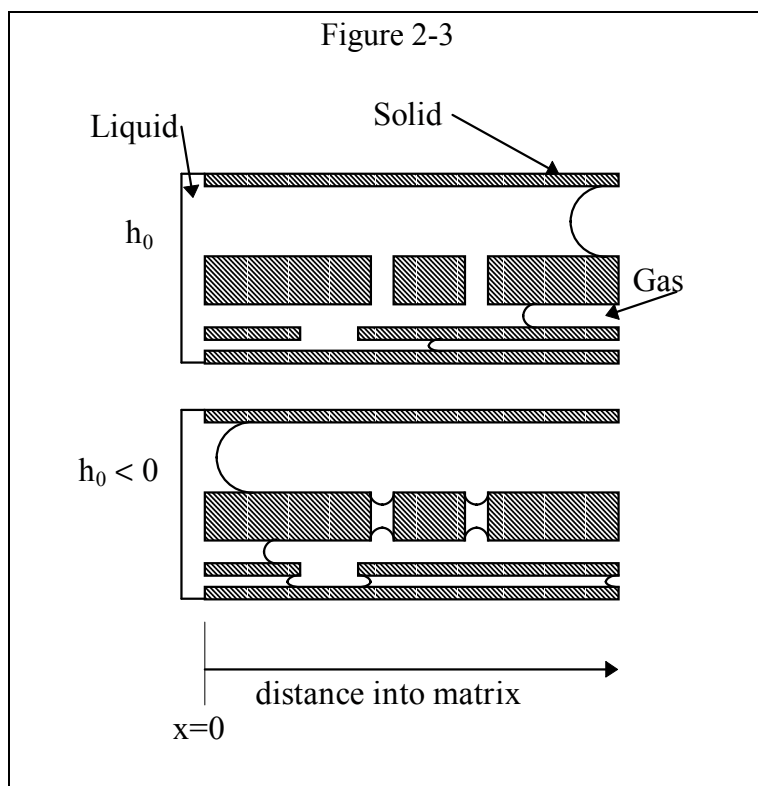
molecular interaction at the liquid interface.

Consider the system in Figure 2-2, where gravity is in the positive y-direction.

When the surface of the fluid in the cup is pierced with a capillary tube, a meniscus will be formed inside the tube with a radius of curvature approximately equal to the radius of the tube. The meniscus will rise in the tube until  $h = h_{\text{suction}}$ , to establish equilibrium in the system. The height of the capillary rise is equal to the suction head generated by the meniscus, as can be proven if a force balance at the meniscus is done following Figure 2-1.



These concepts can be related to liquid flow in soil. By modeling soil as a bundle of capillary tubes, the various effects of capillarity and fluid flow can be taken into account. Refer to Figure 2-3, a representation of a soil system. When the system is first saturated, as shown in the upper part of the frame, water fills all of the void space. If the pressure at the left side of the system is dropped so that there is suction,  $h_0$ , at  $x=0$  in the diagrams, as shown in the bottom part of the frame, water will be drawn back into the



reservoir. Water will be retained in some of the void spaces, however, in a manner relating to Equation 2-4. Water will be drawn out of that particular channel if the suction force of a menisci in the system is less than the suction at the reservoir.

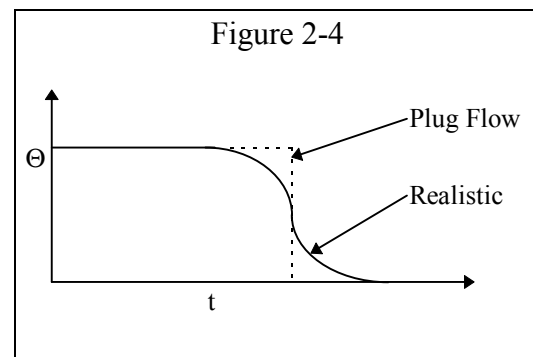
## 2.6: PLUG FLOW

Infiltration has been observed frequently to resemble a plug flow process. Plug flow infiltration involves four criteria in terms of soil water movement:

1. sharp front
2. constant moisture content behind front (in wetted region)
3. constant  $K$  in the wetted region
4. suction head at front

Figure 2-4 compares a plug flow and a realistic moisture content profile graphically. The “realistic” profile shown in Figure 2-4 has been observed by previous researchers (Bruce and Klute, Meyer and Warrick, McBride and Horton, Kao and Hunt). An observation of these researchers has been that the change in moisture content is abrupt, implying that the change in moisture content can be easily approximated with the plug flow assumption as shown in Figure 2-4.

With plug flow, the moisture content profile is a step function, rising sharply from the initial water content to the wetted moisture content. The point at which the moisture content changes from initial to

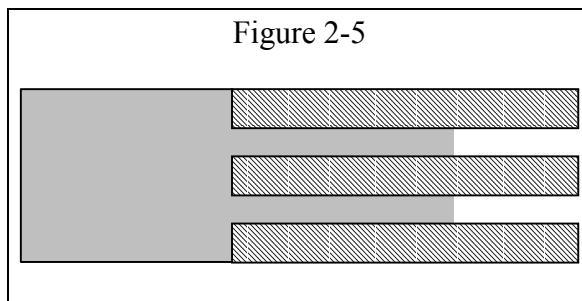


final moisture content is also referred to as the wetting front. Plug flow is not an assumption of complete saturation, but rather one of constant moisture contents in the infiltrated and uninfiltrated regions in which an interconnection exists between the entire bulk of liquid water entering the soil.



The curvature of the realistic profile may not be as pronounced as shown.

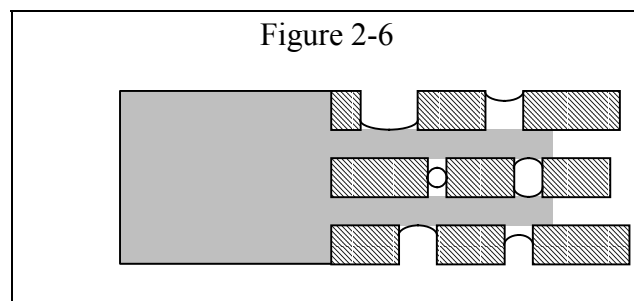
Richard's equation would be well suited to plotting the realistic curve at a particular time, but requires a great deal of data and computation. Unless the exact profile of the moisture content is needed, a simpler model based on a step function may be easier to use. During idealized plug flow infiltration, the "body" of the imbibed fluid is pulled



through the soil by the suction head at the wetting front. This is analogous to flow in a bundle of capillary tubes, as shown in Figure 2-5.

Referring to Figure 2-6, it can be seen how gas pockets can be formed during plug flow infiltration. If infiltration occurs at the same rate in both of the main "channels" shown below, then the gas pockets are formed because the side channels are infiltrated at the same time. Since the gas may not be vented at that time, the complete infiltration of the side channels is effectively prevented by the pressure of the gas in the pocket. Since the model used in this study will assume complete saturation, this reality will be neglected in the quantitative analysis.

Based on the fact that the



capillary effect is driven by a pressure imbalance in the fluid flowing through the soil, it can be postulated that there will be a point at which the wetting front will stop because

the frictional drag of the body moving through the soil will be equal to the suction head at the menisci.

## 2.7: GREEN AND AMPT

All of the concepts presented thus far can be tied together to produce a model for infiltration. In 1911, Green and Ampt developed a simple plug flow model for horizontal infiltration based on the integration of the Buckingham-Darcy Flux Law. This model was based on the assumptions:

- change in moisture content is a step function
- infiltration occurs with a constant head boundary
- $K$  is constant
- $h_f$  has a single value at a sharp wetting front

Where  $h_f$  is the suction head occurring at the wetting front.

The expression for horizontal infiltration in the Green and Ampt Model is :

$$x_f = \left[ \frac{2K(h_0)\Delta h}{\Delta\Theta} t \right]^{1/2} \quad [2-6]$$

where:  $x_f$  = distance wetting front has traveled

$K(h_0)$  = unsaturated hydraulic conductivity based on  $\Theta$  of the wetted region

$\Delta h = (h_0 - h_f)$

$h_0$  = inlet head

$h_f$  = suction head at wetting front

$\Delta\Theta$  = difference between initial and wetted moisture contents

$t$  = time

This model requires a knowledge of the change in moisture contents of the soil.

As with Richard's Equation, such information may be difficult to accurately obtain in the field, thus leading to errors, but approximate errors should be less than obtained when

using Richard's Equation because fewer parameters must be measured. This model also "assumes" that the infiltrating liquid is water through the use of hydraulic conductivity,  $K$ .

## 2.8: POISEUILLE'S LAW

The diameter of the soil pore space varies within the soil matrix. To take into account the different radii in relation to fluid flow, Poiseuille's Law can be applied:

$$Q = \frac{\pi r^4 \Delta P}{8\mu L} \quad [2-7]$$

$$\text{and: } \Delta P = -h_{\text{suction}} \rho g \quad [2-8]$$

$$\text{where: } Q = \text{flow} \left( \frac{L^3}{T} \right)$$

$$r = \text{tube radius (L)}$$

$$\Delta P = \text{pressure drop} \left( \frac{F}{L^2} \right)$$

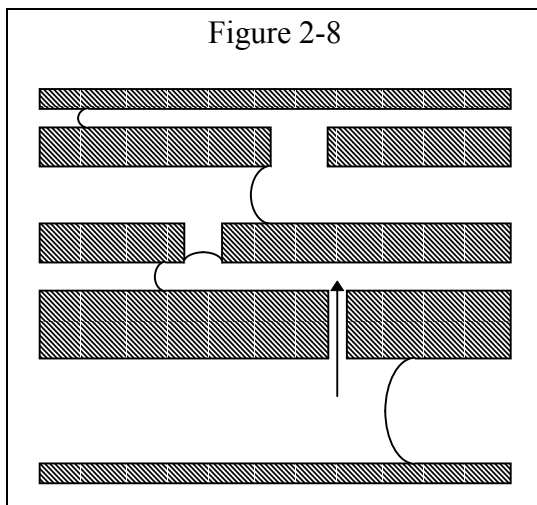
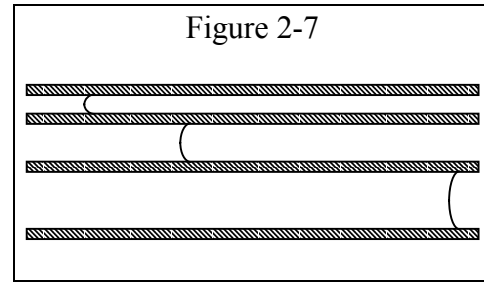
$$\mu = \text{dynamic viscosity} \left( \frac{FT}{L^2} \right)$$

$$L = \text{wetted length (L)}$$

It can be clearly seen that the greater the radius of the pore, the faster infiltration will occur, given that the pressure drop stays the same. Considering the relationship between pore radius and suction head, it can be seen that according to Poiseuille's Law the flowrate will vary by the third power of pore radius. If we model soil as a bundle of capillary tubes, as shown in Figure 2-7, the movement of a liquid through the soil will clearly follow Poiseuille's Law, where the flowrate increases with increased tube radius.

If this bundle of capillary tubes is modified to account for cross-linked channels, as shown in Figure 2-8, the larger channels are infiltrated first, so the larger channels cross

linked to the smaller channels tend to feed the smaller channels. This leads to the



presumption that although flow through the larger channels is faster, the smaller channels are flooded as a consequence of the assumption that all pores in the soil matrix are interconnected.

## 2.9: KAO AND HUNT

Although the Green and Ampt Model works fairly well, it still requires field measured data. In 1996, Kao and Hunt derived a model by integrating Poiseuille's Law with capillary suction head to arrive at:

$$x_f = B \left( \frac{\sigma}{\mu} \right)^{1/2} k^{1/4} t^{1/2} \quad [2-9]$$

where:  $x_f$  = distance between the inlet and the wetting front

$B$  = a function of the soil geometry

$\sigma$  = liquid surface tension

$\mu$  = liquid dynamic viscosity

$k$  = permeability

$t$  = time

Although the model may not be as theoretically rigorous as Richard's Equation, it requires less parameters and is easier to solve. The parameter  $B = 0.5$  is an empirically determined constant based on an extensive review of published experimental data (Kao and Hunt, 1996). The parameter of time is the independent variable of the equation, and the permeability can be determined experimentally. Surface tension and viscosity are either measured or looked up. This model gives a reasonably accurate value for the wetting front movement for a variety of soil types and is valid for horizontal, initially dry soil. It has been shown to be in good agreement with experimental data.

#### **2.10: TEMPERATURE EFFECTS ON THE KAO AND HUNT MODEL**

The Kao and Hunt model was experimentally verified for a narrow temperature range of 20 to 24 °C. However, the range of temperatures that may be experienced in the environment varies a great deal. Therefore, a logical step in the analysis of the Kao and Hunt model is to test the sensitivity of the model to different temperatures and to verify whether or not the model can predict changes in the temperature.

The seasonal variation of soil temperature has been a well studied phenomenon. Smith(1932, Cited in Jury and Gardner 1991), noted a temperature variation of about 10 °F (about 5.6 °C) in California at a depth of eight feet, fluctuating more at shallower depths. The variations peaked at about 90 °F (about 32 °C). Pearce and Gold (1959) noted a temperature variation of about 20 °C at a depth of 10 cm in Ottawa, Canada. The minimum temperature observation of that study was about -4 °C.

Looking at the Kao and Hunt model, it can be seen that two of the parameters, surface tension and viscosity, are functions of the liquid infiltrating the soil. These parameters are also known to change with temperature while other parameters are functions of soil geometry and are independent of temperature.

These simple observations lead to the question of whether or not an adequate adjustment of the model for various temperatures can be obtained by simply inserting the values of temperature and viscosity corresponding to temperature. If the surface tension and viscosity are the governing temperature sensitive parameters, then this adjustment may be enough to account for most temperature effects. Thus, if the model can be adapted for various temperatures, then changes in the temperature will result in a variation in  $x_f$ .

#### *2.10.1: VISCOSITY*

Viscosity is the resistance of a fluid to a shear force. If a plate is dragged over a film of fluid, the frictional drag of the fluid is described by the relation:

$$\tau = \mu \frac{du}{dy} \quad [2-10]$$

where:  $\tau$  = shearing stress

$\mu$  = dynamic viscosity

$\frac{du}{dy}$  = change in fluid velocity with distance from the conduit wall perpendicular to the face of the plates

(Munson 19)

The parameter viscosity is the slope of a plot of shearing strain vs. shearing stress. The higher the viscosity of a fluid, the greater the force required to deform a body of the fluid. For example, molasses at room temperature has a higher viscosity than liquid water.

Most basic fluid mechanics books will report the viscosity of water for a variety of temperatures. A fairly good mathematical relation for the viscosity as a function of temperature is the equation(Reid 388-490):

$$\ln \mu = A + \frac{B}{T} + CT + DT^2 \quad [2-11]$$

where:  $\mu$  = dynamic viscosity

$T$  = temperature (K)

and for water:  $A = -24.71$

$B = 4209$

$C = 0.04527$

$D = -3.376 \times 10^{-5}$

The result of this equation is the dynamic viscosity in centipoise. The output from this equation is in good agreement with tabulated values. This formula is presented to show that the viscosity is a function of temperature and could be directly computed directly provided that the temperature of the system is known.

### ***2.10.2: SURFACE TENSION***

Jasper(1972) provides a compilation of the surface tensions of about 2200 pure liquid compounds. The surface tension of water was reported to vary following the equation:

$$\sigma = a - bT$$

[2-12]

where:  $s$  = surface tension(dyne/cm)

$T$  = temperature (degrees C)

and for water:  $a = 75.83$

$b = 0.1477$

This equation and reported values have a degree of error of  $\pm 0.10$  dyne/cm. As can be seen from Equation 10, the surface tension varies linearly with temperature. The range of reported values was 10 to 100 °C.

### ***2.10.3: OTHER EFFECTS***

As a part of understanding some of the other processes that may be occurring in infiltration, a simple conceptual diagram is shown in Figure 2-9.

where:  $Q_R$  is the flow from the reservoir

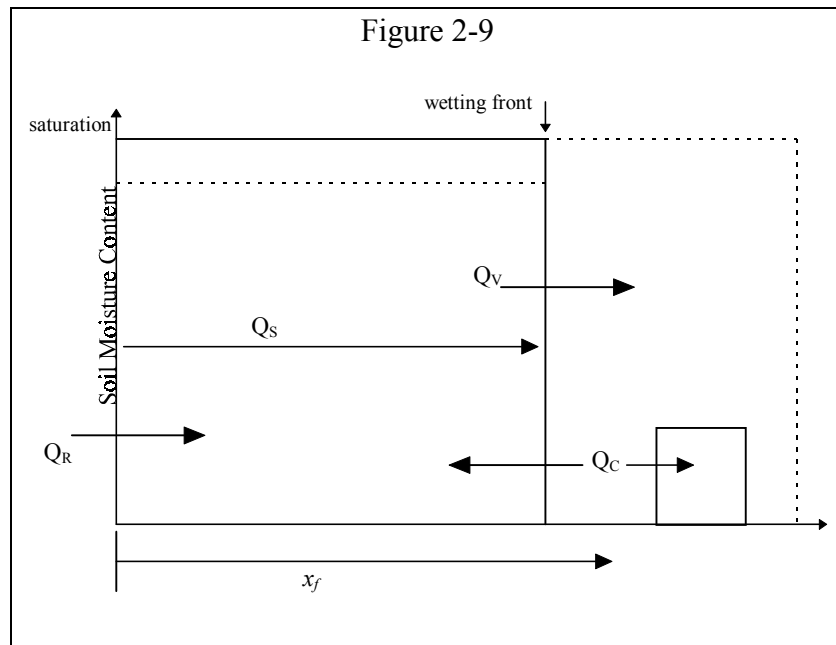
$Q_S$  is the flow into the soil matrix

$Q_V$  is the vaporization of liquid

$Q_C$  is the condensation of the liquid back into the soil matrix



The liquid enters the soil matrix at the left and travels towards the right ( $Q_R$ ), so that  $x_f$  increases over time. At the interface between the liquid and gas phases, an



evaporation/condensation process will occur. [If a liquid is in equilibrium with its headspace, then the rate of evaporation equals the rate of condensation.] Thus a vapor cloud(not really shown in Figure 2-9), will form to the right of the liquid front as shown above.

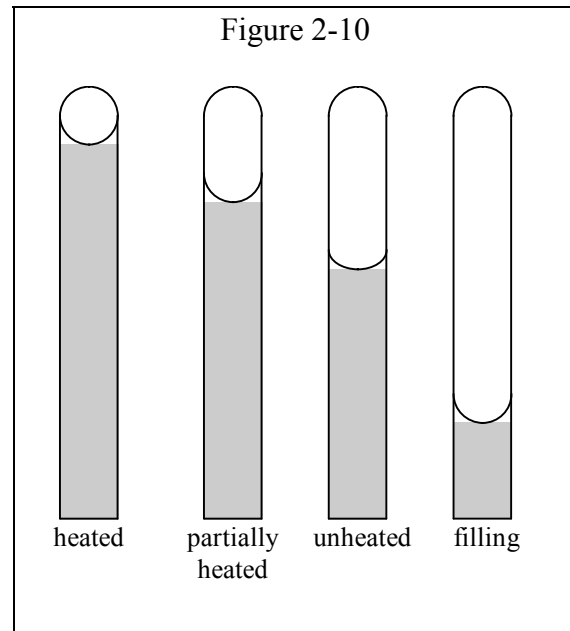
If the temperature of the soil matrix is below the dew point(the point at which vapor will condense) of the vapor, the vapor will condense( $Q_C$ ) in the soil matrix ahead of the wetting front. The specific heat of soil solids is low compared to that of the latent heat of water, so condensation of water will tend to heat the soil solids.

In the case of water as infiltrating liquid, the effects of condensation and evaporation will not affect the wetting front movement, therefore the Kao and Hunt Model will not be modified to address condensation and evaporation.

Thermal expansion of the infiltrating liquid may not contribute to the movement of the wetting front. This statement is based on two facts:

1. Infiltration with partial saturation can occur, as explained in Section 2.6
2. If a liquid is heated, its density will decrease.

Consider the infiltration process as analogous to filling a series of thermometers with mercury, as shown in Figure 2-10. The thermometer tubes represents the void space in the soil. The thermometers are filled to the same level in identical tubes, representing a consistent final moisture content. If the tubes are heated, the volume of the



mercury will increase within the tube. This is similar to the expansion of the infiltrating liquid into unfilled void spaces; the partial saturation leaves room for the expansion of the infiltrating liquid.

The vapor pressure also depends upon temperature, which in turn affects evaporation and condensation. A liquid of appreciable vapor pressure will tend to evaporate, and can be transported in the vapor phase. If the vapor pressure is high enough, the liquid in the wetting front will be evaporating from the face of the front. If the flux rate from the face is equal to or greater than the imbibition rate induced by the

front movement, then the wetting front will appear to slow down, stall, or back up. For a liquid such as water which tends to evaporate fairly slowly, this effect may be negligible, however, for hydrocarbon fuels and other liquids with very high vapor pressures, this effect may be very pronounced.

#### ***2.10.4: WHAT PARAMETERS SHOULD NOT CHANGE WITH TEMPERATURE***

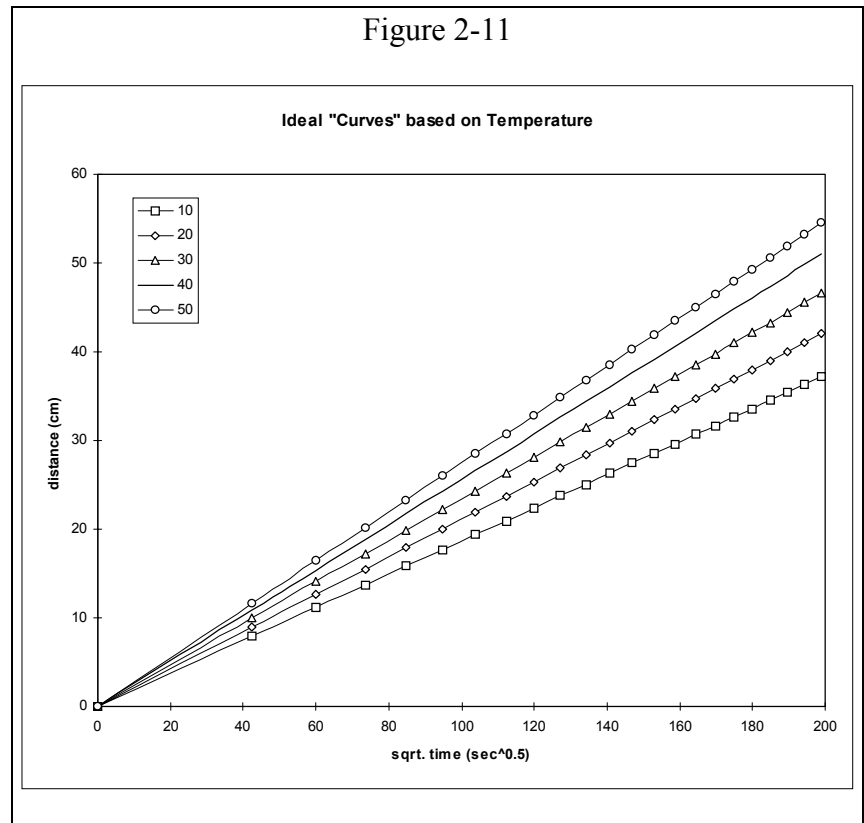
Some parameters in the model are not temperature dependent. Looking at the Kao and Hunt Model(Equation 2-6), two of the parameters:

- B
- permeability

are the effects of the soil matrix geometry on fluid flow. The B parameter is an experimentally derived constant determined through an extensive review of published data(Kao and Hunt). Given that the value of 0.5 applies to most any type of soil, it is likely that B is independent, or very insensitive to, temperature. The permeability of the soil should generally not change due to temperature differences because the change in density of silicon dioxide should be insignificant at the temperature range in question.

### 2.10.5: SENSITIVITY

Given that the Kao and Hunt model uses parameters that depend upon temperature, it can be postulated that the model is sensitive to temperature. Knowing the values of viscosity and surface tension for different temperatures, the Kao and Hunt model can be run for a range of temperatures with the hypothetical soil sample described earlier. The model predictions for a



temperature range of 10 to 50 °C is shown in Figure 2-11. The figure shows a noticeable change in the predicted rate of infiltration in the hypothetical soil sample. The infiltration rate is not very large so large variations in  $x_f$  are not expected.

### **3: EXPERIMENT**

In this chapter, the experimental variation, procedures, and equipment used in this study will be described.

#### **3.1: EXPERIMENTAL VARIATION**

This study sought to observe the change in the movement of the wetting front through soil under different temperatures. As with any experiment, one parameter is changed to isolate the effect of the parameter. The change in the temperature used for this study was based on a combination literature review and laboratory feasibility.

A laboratory experiment is limited to the conditions that can be replicated in the lab. To make the apparatus simple, the temperature variation used in the experiment was:

- Scenario 3: cool, about 10 °C
- Scenario 1: lab temperature, about 20 °C
- Scenario 2: warm, about 30 °C

The temperatures mentioned were target temperatures, during the experiment the actual temperatures were measured. The cool target temperature is based on the way water freezes. As the temperature drops from 4 °C to 0 °C, the density of water drops as the molecules align into a crystal structure. Laboratory room temperature was used as a “control” in the infiltration experiments. The warm temperature was based on the high natural temperature as based on the literature review(see Section 2.10).

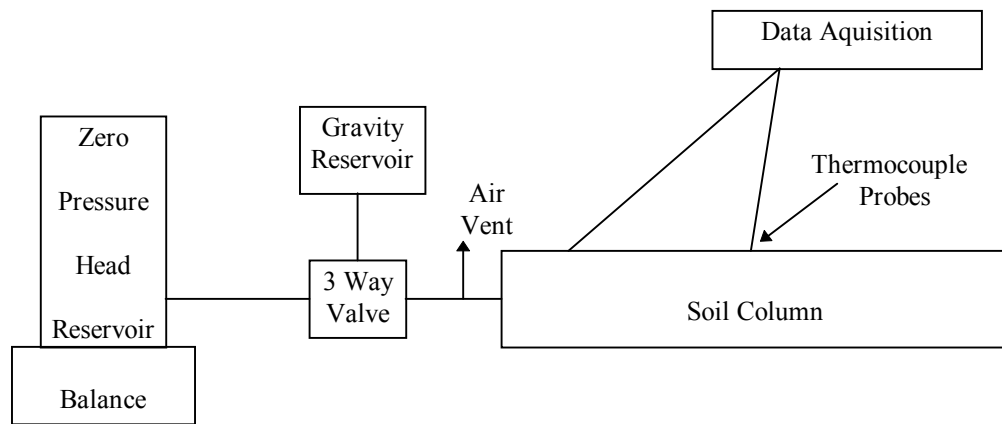
### **3.2: EXPERIMENT APPARATUS**

The design of the experimental apparatus used in this study was borrowed from other research. This was done for consistency and to reduce the effort required to develop the experiments. For the most part, the apparatus used was based on the apparatus developed by Bruce and Klute, 1956. Minor changes to the design were done by Kao and Hunt in 1996.

#### **3.2.1: *WHOLE SYSTEM***

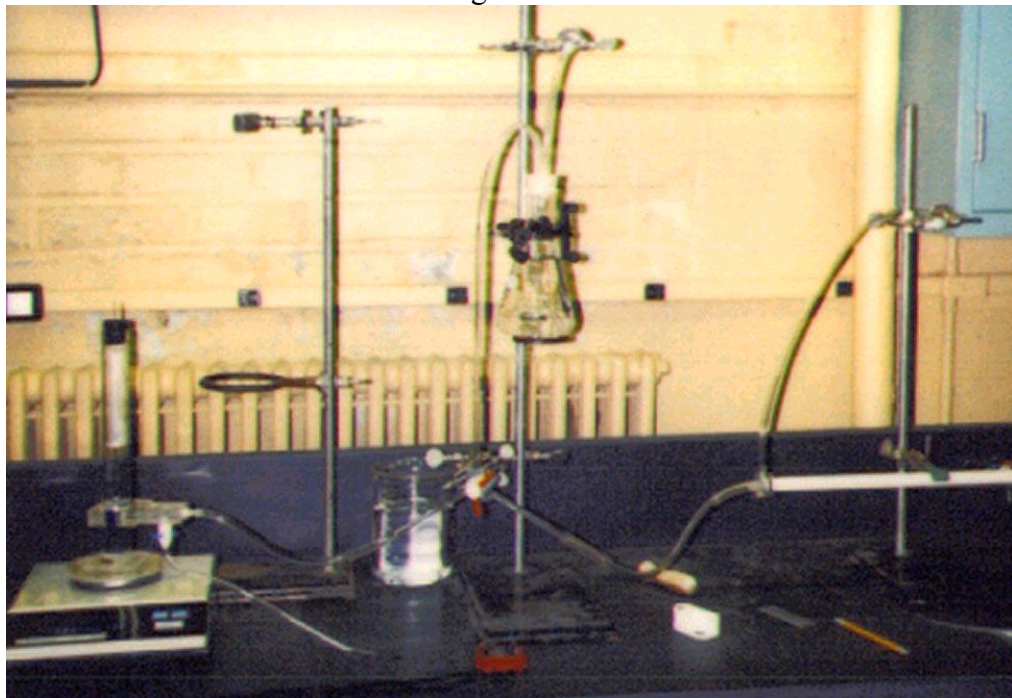
In general, the entire experimental system is outlined in Figure 3-1. Before the experiment is run, the system is dry. The plumbing system is loaded with water using a gravity reservoir, which is linked to the system through a three way valve. The Zero Pressure Head reservoir was used to deliver water to the soil column. The thermocouples and data acquisition were used to record the temperature of the soil column at regular intervals. Figure 3-2 is a picture of the basic setup. In this picture, the basic parts of the experiment, with the exception of the thermocouples and vacuum chamber, can be seen.

Figure 3-1: Whole System



This diagram above follows the photo shown below. The balance is at the lower left, the gravity reservoir is on a stand at the center, and the soil column is held by a stand and clamp at right. Data Acquisition was not shown for clarity.

Figure 3-2

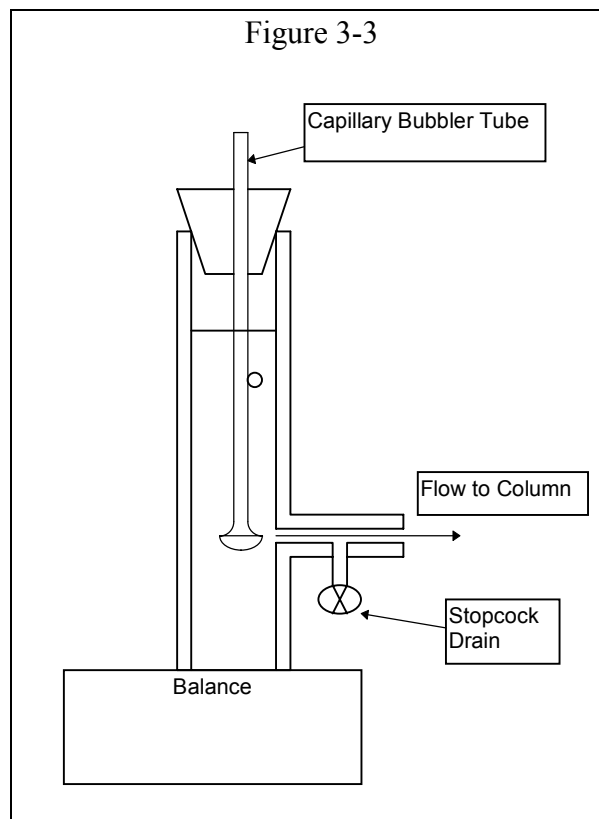


### 3.2.2: ZERO PRESSURE HEAD RESERVOIR

The Zero Pressure Head Reservoir, shown in Figure 3-3 is used to deliver fluid to the soil column during infiltration without applying fluid pressure to drive the infiltration front through the soil. Zero pressure at

the column inlet is maintained with a small reservoir with a bubble tube. As infiltration occurs, air is introduced into the headspace of the reservoir.

Since there is air within the capillary bubbler tube down to the bottom of the tube, the pressure within the reservoir is at atmosphere at the bottom of the reservoir. It thus becomes a matter of leveling the bottom of the capillary bubbler tube with the center line of the



soil column and water will be infiltrated at zero gauge pressure. Some more conventional applications and configurations of the Mariotte bottle are shown in Rowell(1994).

### 3.2.3: SOIL COLUMN, CAPS, AND THERMOCOUPLES

The soil column is a cut length of acrylic tubing. Two sets of columns were used, some with thermocouple ports and some without thermocouple ports. The ports were used to attach the thermocouples to the column.



Figure 3-4

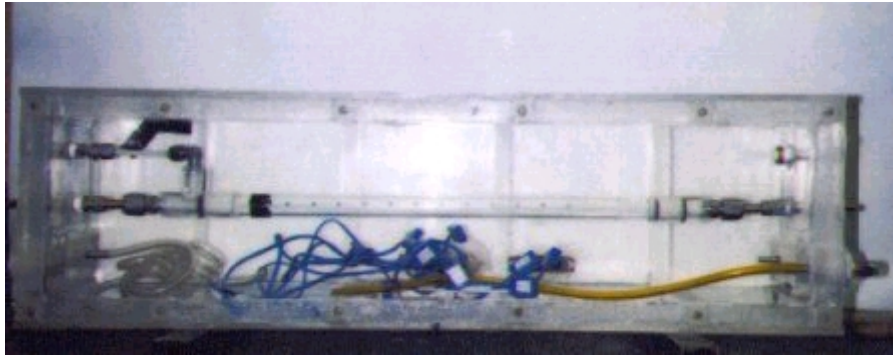


Figure 3-4 shows the soil column as mounted in the vacuum chamber. The thermocouples have been removed for clarity, but the thermocouple jacks can be seen at the bottom of the box. The holes for the thermocouples can be seen in the middle of the soil column.

There were two different types of caps. The caps were constructed of machined acrylic with fittings and o-rings. The head cap is shown in the schematic Figure 3-5 and in the photograph Figure 3-6. The reservoir and vent in the cap allow for the purging of air from the system during the initiation and the even distribution of water along the vertical face of the soil column. As a result of this, water is infiltrated in a fairly even plug through the column.

Figure 3-5

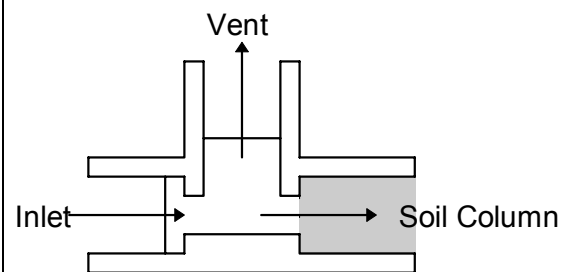


Figure 3-6

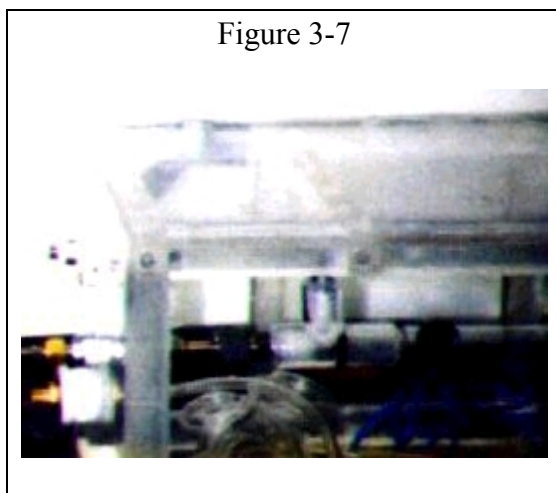


The caps were made with fittings to make connection to the plumbing system of the vacuum chamber. Face seal fittings were used at the inlet of the caps to connect the cap to the reservoir and to hold the column in place in the vacuum chamber, described in the next section. They provided adequate structural rigidity and provided a fairly reliable and leak free connection.

Thermocouples were used to check for an even temperature distribution during the infiltration and to check for the temperature spike that has been found to be an interesting phenomenon associated with the wetting front (Anderson, et al 1962). Each thermocouple was mounted inside a #6 stainless steel machine screw. Stainless steel was used because it was the same “neutral” metal used in the screws of the plug, stainless steel does not adversely affect a thermocouple it contacts. The screw was then mounted to a standard subminiature thermocouple wiring plug. The thermocouple was held in place by a blob of 5 minute 2-part epoxy. This provided a smooth, neat, strong, and watertight product that could be tested using a hand held microprocessor thermocouple thermometer. Holes were drilled into the soil column at one inch intervals along its length, and the thermocouple screws were then screwed into these holes until the thermocouple tip just protruded into the soil.

### 3.2.4: VACUUM CHAMBER

In order to insulate the soil column, a vacuum chamber was constructed. The vacuum chamber is most notably shown in Figure 3-4 and Figure 3-7. Figure 3-7 more clearly shows the construction of the chamber.



The vacuum chamber was made of acrylic and sealed using Silicone sealer (the type that releases acetic acid when it cures). “Snoop” brand leak detector was used to check for leaks. All of the ports required through the chamber walls were either cemented in place with five-minute epoxy

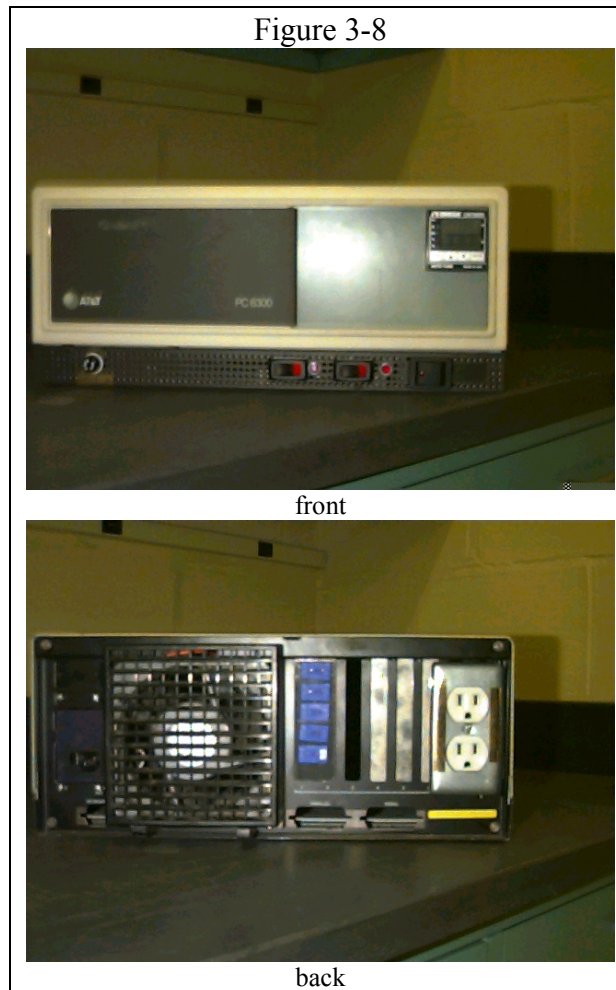
and sealed over with silicone, or fitted in using NPT standard pipe fittings sealed with Teflon tape. The pipe fitting holes were duplicated on the opposite side of the chamber wall, so that bulkhead type fittings were not used. The front panel of the chamber was bolted on to allow access and mounting of the soil column. The front panel was sealed using a cast-in-place silicone gasket and vacuum grease.

In hindsight, the use of NPT pipe fittings is ill advised when a precise fit is required. Since the NPT fitting is slightly tapered, the depth of the thread tap determines the effective length of the fitting. It would have been much easier to use straight thread fittings with seals than NPT fittings.

### 3.2.5: CN76000 TEMPERATURE

#### CONTROLLER AND ASSOCIATED HARDWARE

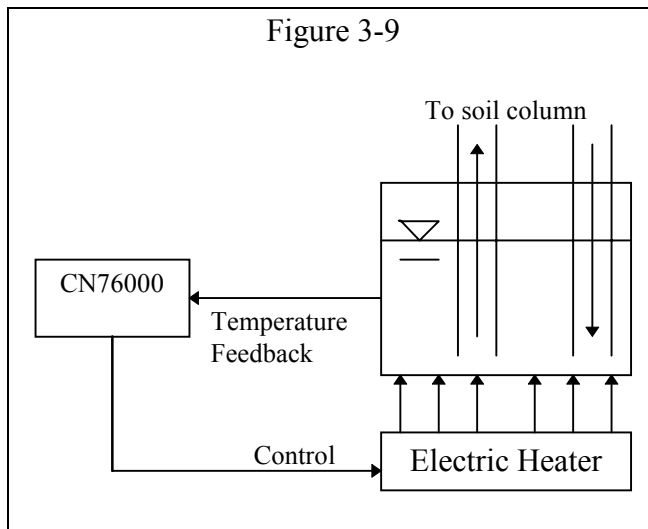
A CN76000 Self Tuning temperature controller (obtained from Omega Engineering) was used to control the temperature of the column by driving the devices used to heat and cool the column. The controller was mounted in the case of a gutted 8086 personal computer, which provided a solid and spacious mount and wiring box. The controller was set up to drive a solid state relay mounted to a heat sink.



This enabled the CN76000 to directly control the hot plate for the heater bath. Figure 3-8 shows the resulting hardware.

### 3.2.6: HEATER

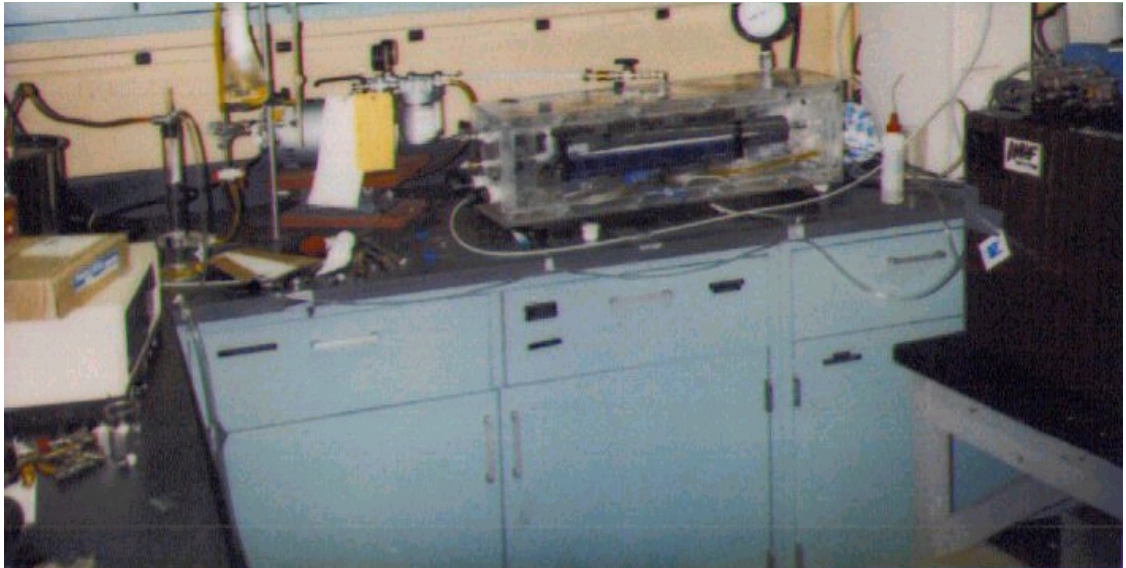
The heater apparatus consisted of a conventional electric heater element, a 12 quart stock pot, and copper tubing. After equilibrium was established, the soil column temperature was constant but lower than the reservoir temperature due to losses from the uninsulated tubing and heat transfer to the column from the tubing.



The element was controlled by the CN76000, and the temperature reading was taken either at the water bath or at the head of the column. It was found that the CN76000 had finer control of the water temperature if the temperature feedback came from

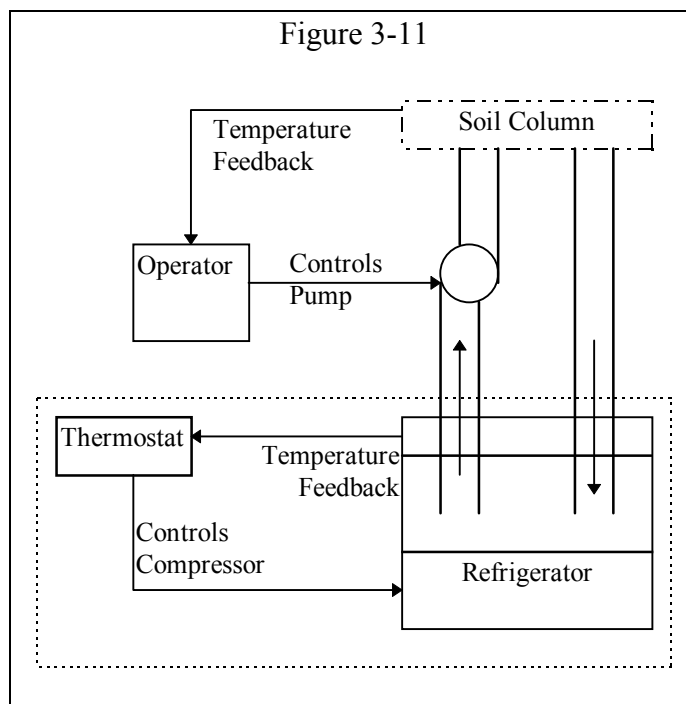
the mass of the water bath rather than the head of the column. The temperature of the water bath was maintained at 100 °F. Figure 3-9 is a schematic of the heater system. The heater can also be seen in the far left of Figure 3-10.

Figure 3-10

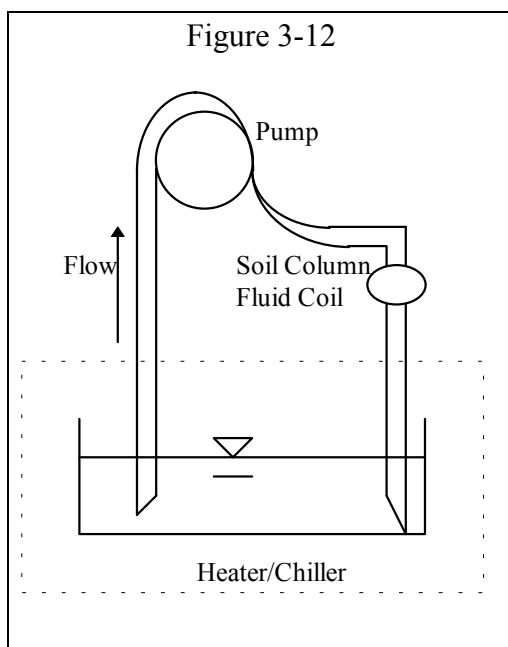


### 3.2.7: CHILLER

The chiller bath consisted of an open reservoir stored in a General Electric 1.5 cubic foot refrigerator. The temperature and flow of the cold water was manually controlled. Since the refrigerator has a hard wired thermostat, the ideal solution would have been to rewire the



refrigerator so that the thermocouple reading used to control the compressor could be selected. Doing so would make the refrigerator work in a manner much like the electric heater element, however, this may have damaged the compressor with a short cycle time. The refrigerator was kept at its lowest setting. This kept the water bath close to but not much lower than 0 °C. The reservoir was a food storage container, which was placed in the small “freezer” section of the refrigerator. The temperature of the reservoir water was periodically monitored using a thermocouple thermometer. The temperature ranged from 0 to 10 °C. This thermocouple probe was used to “balance” the flowrate and temperature of the chiller water. A schematic of the chiller can be seen in Figure 3-11, and a the chiller can be seen at the right-hand side of Figure 3-10.



### 3.2.8: FLUID PUMPS

Lab scale peristaltic pumps were used to move the coil fluid. Peristaltic pumps were used because they are self-priming, can be used without contamination or heating problems, and were readily available in the laboratory. The pumps were used as part of a recirculation system, where the fluid was drawn from an open tank (the stock pot for the heater and the food container for the chiller) and dumped back

into the open tank. A conceptual diagram of the setup is shown in Figure 3-12.

This setup was convenient also because it was easy to drain and load the fluid coil. By removing the suction end of the tubing, the pump would run the system dry. Fluid normally stored in the tubing would be transferred to the reservoir, and because the reservoirs were large in comparison to the volume of fluid stored in the tubing the reservoirs could hold the extra fluid. In a similar way, the system purged itself of excess air quite rapidly, as the suction end of the system always draws fluid from the bottom of the reservoir.

### **3.2.9: DATA ACQUISITION COMPUTER**

Thermocouple readings were taken using a data acquisition computer. The acquisition board, a CIO-DAS 16, was installed in a Pentium 133 IBM Compatible PC. A CIO-EXP32 signal conditioning board was used to connect the thermocouples to the DAS16. Labtech Notebook for Windows was used to set up and run the experimental data collection. Data was collected at a rate of 0.1 Hz.

This system worked well for the intended purpose. A simple modification to the benchtop signal conditioning board was required for thermocouple use, but the necessary signal amplification, cold junction correction, and open detection functions were present on the board. The MS Windows based software featured drag-and-drop application design which made setting up and modifying data collection routines simple. The computer was set up to write all of the collected data to a delimited text file, so that the data could be read into a spreadsheet (MS Excel was used, but most spreadsheets should have this capability).

### **3.3: EXPERIMENTAL PROCEDURES**

The procedures for setting up and conducting the experiments will be described.

In general, the procedure was:

- prepare the soil sample
- “mount” soil sample in testing equipment
- run experiment

The procedure was straightforward, but will be described in a fair amount of detail.



### ***3.3.1: SAMPLE PREPARATION***

The first step in testing the soil is to prepare a soil sample. To maintain uniformity, a regular procedure was followed in the preparation of the sample, which will be described here.

#### ***3.3.1A: PACKING***

The silica powder was dispensed from a beaker into the column using a peristaltic pump. Contamination of the soil by the tubing used was assumed to be negligible or equal to the contamination from any other laboratory packing utensil that could have been used. The pump action crushed the tube to move the powder, and running the pump dry or with silica powder tended to overheat the tubing, subsequently distorting and discoloring the tubing. Although the tubing was flattened and discolored where it was in service, damage was restricted to the length of the tubing in contact with the pump rollers. In comparison to the mass of soil moved by the pump, the amount of tubing contaminating the soil sample would be slight.

The column was packed in multiple lifts. After weighing the column, soil was pumped in, then the weight was taken again. The height in the column for a lift was then estimated based on the desired dry bulk density and the weight of soil added. The soil was then packed with an acrylic rod and the true bulk density was determined by measuring weight and height. Packing the column in this way allowed the operation to be done quickly and neatly without a spillage factor to affect the quality of the packing. In

other words, it was easier to pack the soil column in this way rather than to attempt to put a pre-weighed sample into the column.

### *3.3.1B: PLUGGING WITH MACHINE SCREWS*

After cleaning, the column was refitted with machine screws for packing. This was done to prevent spillage during packing without the possibility of damaging the thermocouples. The sides of the screws were smeared with vacuum grease and carefully screwed into the column. Care was taken to not cross threads because the stainless steel screws would tear the acrylic column. The screws were inserted so that the tip of the screw was flush with the inner wall of the column. After plugging, a small ball of paper towel was passed through to wipe out most of the vacuum grease that was forced into the column by the action of the screws.

The caps were slid onto the column and sealed with vacuum grease. The grease was placed on the column so that the amount of grease pressed onto the wire screening would be minimized. The caps were “furred out” with acrylic inserts and o-rings to extend the soil column so that it would fit snugly in the vacuum chamber. A wire mesh screen was used to prevent the soil from spilling into the cap reservoir, and was not separated from the column by an o-ring. Care was taken not to scar the soil sample, as a smooth and flat interface at the head of the column is desired.

The thermocouples were then fixed to the column using the same procedure that was used to place the screw plugs. The thermocouples were added before the

permeability test because the extra matter at the tip of the screw may have locally compressed the soil.

#### *3.3.1C: CONTINUITY TEST FOR LEAKS*

After plugging all the holes, the empty column was continuity tested for leaks. Using the air permeameter, the flowrate into the column was matched to the flowrate out of the column. If the flows were about the same, based on timing the bubble flowmeter, the column was then considered to be adequately plugged. Also, since the air from the permeameter was clean and dry, it can be assumed that most of the residual moisture in the column was removed by the air flow.

#### *3.3.1D: END PREPARATION*

After continuity testing, the endcaps were removed from the column. The vacuum grease used to seal the caps was wiped off. One end of the column was closed with a double or quadruple layering of Parafilm and electrical tape. Sometimes, an o-ring was placed on the end to help hold the temporary seal in place. The Parafilm is an adhesiveless, pure plastic that spanned the end of the column like a drum skin, while the electric tape helped prevent breakage during packing.

### *3.3.1E: PERMEABILITY TEST*

The permeability test was performed after the endcaps and wire screens were placed on the column. The soil column was hooked up to the permeameter through the endcaps. This provided a solid mechanical connection for the test, and since the fittings were of high quality leakage from the fittings was assumed to be negligible. The soil column was then tested for permeability. The permeability setup, procedure, and formulae are summarized in the Appendix.

### *3.3.1F: CLEANING*

After each use, the column was cleaned of residual grease, soil, and moisture. This was done to ensure that the packed column would be consistently clean. After removing the column from the apparatus, all thermocouples and screw plugs were removed.

The next step was to remove the endcaps from the column. Residual water was shaken and wiped out of the endcaps. The wire mesh screens were then removed, and the endcaps were placed in a dissector to remove all remaining water. This was done to prevent a premature initiation of wetting by any remaining water.

The screens were cleaned using store bought rubbing alcohol(isopropyl). The primary contaminant of the wire screens was vacuum grease, which is not water soluble and easily clogged the mesh. Rubbing alcohol was found to dissolve vacuum grease quickly and was thus used as a cleaning solvent. Screens were placed in an Erlenmeyer

flask and stirred quite vigorously using a magnetic stirrer. This cleaning usually required about ten to twenty minutes.

Most of the soil was removed from the column by violently swinging the column over a waste container or hitting the waste container with the column. In some cases the powder could be pushed out using a rod or washed out with distilled water. No attempt was made to recover the used powder because wetted and dried powder had a cement-like nature when re-dried. In some cases, a plug was taken from the head of the column and dried to verify the dry bulk density of the soil in the column.

The column was brushed out and washed using hot water and laboratory detergent. This removed soil and residual vacuum grease from the column holes. At times, rubbing alcohol and Lava hand soap were also used. The column was dried by pushing a small ball of paper towel through with a rod. This produced an adequately clean interior surface. Extra care was taken to remove any remaining vacuum grease, as this would affect the wetting properties of the materials in contact with the “experimental region” of the apparatus.

### ***3.3.2: SETTING UP THE EXPERIMENT***

After the permeability test, the column was mounted in the vacuum chamber for the experiment. Before sealing the chamber, the thermocouples were connected to the computer board wiring harness and the computer data collection program was run to check for proper operation of the thermocouples. This was to make sure that most, if not all the thermocouples were working. If one or two thermocouples were malfunctioning

usually they were just ignored. If required, the water coil was wrapped around the column and the ruler was aligned.

The vacuum chamber was then evacuated to the normal operating pressure of about 5 PSI and the soil column was checked for air movement using leak detector. If the column fittings were not properly tightened, the column would leak the vacuum. This situation was undesirable because the negative vacuum pressure leaking into the tail of the soil column is equivalent to a positive pressure head at the reservoir. It was found that due to leakage through the slide seal between the soil column tube and cap that the vacuum chamber would not hold vacuum. In the end, the vacuum chamber was closed, but not evacuated, to limit heat gain and loss.

After the soil column was properly sealed, the outlet on the Mariotte bottle and the inlet on the vacuum chamber was aligned using a spirit level. If the two were found to be out of level, they were shimmed to the proper position.

### ***3.3.3: INITIATION OF THE EXPERIMENT***

The steps taken to initiate an experiment were to:

- make sure everything is in place
- open vent ball valve
- flood head cap chamber with siphon reservoir and start timer
- close ball valve when water starts leaking out and simultaneously close off the siphon reservoir
- connect zero pressure head reservoir to the column

These steps are self explanatory. The picture of the experiment clearly shows all of the parts of the plumbing system.

#### **3.3.4: ENVIRONMENTAL CONTROL**

The environment that the soil column is in was controlled. The experiments were performed in an air-conditioned room, where the temperature varied a few degrees. In comparison to the time of the experiment, the resultant temperature wave over time was small.

The vacuum chamber and insulation was used to insulate and isolate the column from the room atmosphere. Although the vacuum chamber was not evacuated during most of the runs due to the technical problems with sealing the column, the chamber was considered to be effective in preventing heat transmission due to air currents in the room. The vacuum chamber was also used to mount the column in a fixed and level position. The column was further insulated using a length of foam pipe insulation. This insulation is inexpensive and available in a range of sizes. Since the insulation was factory split, it was easy to install on the mounted column.

#### **3.4: TECHNICAL PROBLEMS WITH USING VACUUM**

The experimental apparatus was meant to be reusable and vacuum tight. The vacuum chamber was reusable but was not able to continually hold vacuum. This was discovered because the vacuum chamber required continuous suction, rather than being able to hold vacuum. This may have been overcome by using permanently mounted thermocouples or by using a tapered thread for the thermocouple ports.

The chamber was put under vacuum and both ends of the column were checked for air flow using a loop of tubing and water. The column was sucking air, which

indicated a leak to the column through the vacuum chamber. In checking the column, the thermocouples were loose. Since the screws were straight thread and not tapered thread it does make sense that the screws could not hold the pressure(2.45 PSI), but the continuity test did not pick this up because the tail end flowmeter was a bubble flowmeter, which vents to atmosphere.

Modifications to the soil column were made to accommodate vacuum work. When using the vacuum, it was found that the soil column was leaking. The most plausible reason for this was that the straight threads and vacuum grease was not sufficient to seal the column against the vacuum. This phenomenon was identified using a small loop of tubing filled with water; when attached to the column inlet and outlet vents with vacuum the water was drawn up into the column.

### **3.5: CONCLUSION**

The apparatus described in this chapter was used to run fourteen experiments. The data from these experiments is reported in the next section. This is followed by a detailed discussion of the data and its relation to the model.

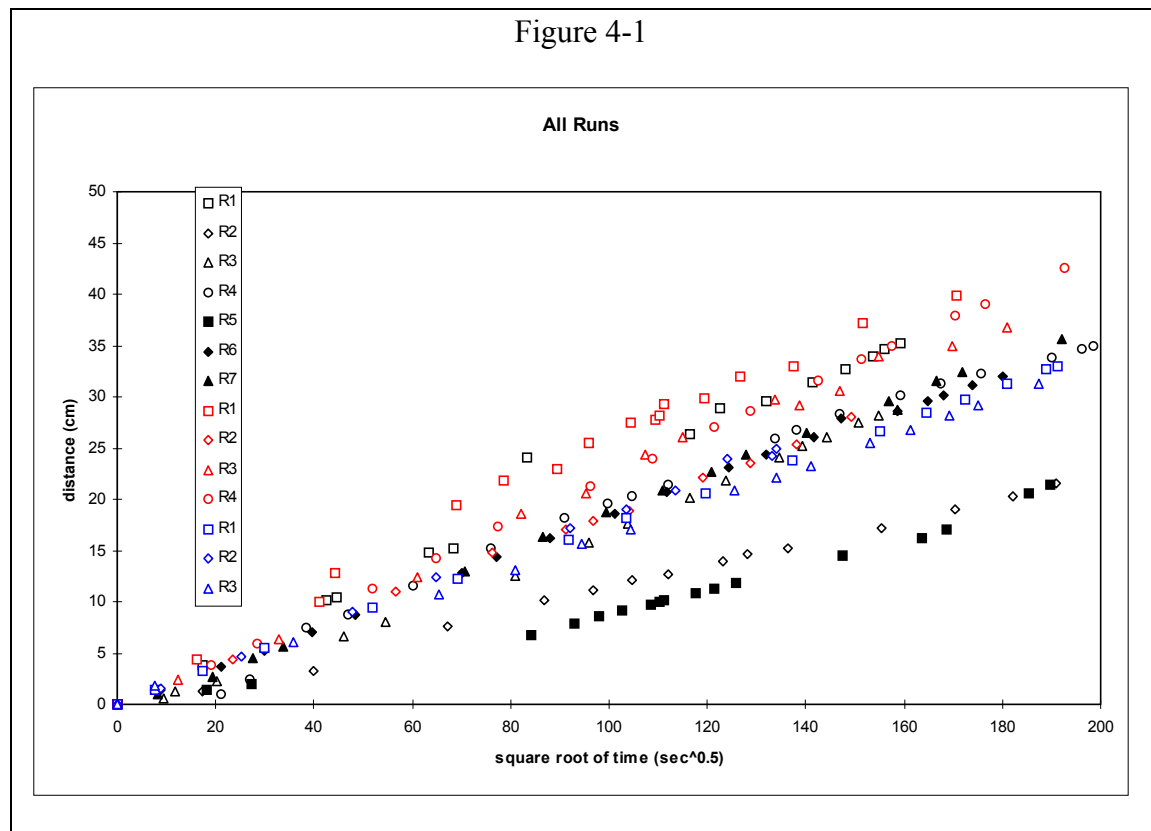


## 4: PRESENTATION OF DATA

In this section, the experimental data will be presented. The model predictions along with the experimental data will be graphed together. The process by which the data was refined will also be shown. The data was collected in sets, each set representing a separate experimental run. The runs are numbered sequentially based on the scenario and the run number.

### 4.1: ALL DATA

Using the experimental setup described in the previous chapter, data was collected during a series of experiments. The results of all of the experiments done are



shown in Figure 4-1. Individual data points are represented by symbols. The data is labeled based on the run number and color coded depending upon the temperature range used. As can be seen from the data, there is some disagreement between the runs as to the effect of temperature on the wetting front movement. This leads to the conclusion that there are either complicating factors in the problem that are not being taken into account or that some of the experimental runs were not properly completed.

The gathered data set was purged of unreliable data. This was based on known physical problems with a particular experiment. Physical problems with experiments included:

- vacuum leaks
- plumbing problems
- restarts
- packing inconsistencies

All of these problems have an adverse effect on the lab data when compared to the model.

A vacuum leak into the soil column can have an effect on the wetting front. Suppose that a vacuum pressure of 5 cm of water is applied to the chamber, and that it is known that the soil column is leaking. This situation is essentially the same as 5 inches of pressure head at the inlet side of the system. The few times that vacuum was used as insulation during an experiment, there was not a remarkable change in the rate of infiltration. This may be due to the low permeability of the soil; the air flow from the tail vent of the column would be restricted by the small channels.

Plumbing problems included:

- bubbles in the feed lines
- backpressures
- leaks

Bubbles in the feed lines can effectively cut off the flow of fluid through the inlet and affect the rate of imbibation. In theory, the bubble will be dragged along by the imbibation and float out of the way when it reaches the cap reservoir. Since some parts of the feed line were opaque, it was impossible to tell if a bubble had “hung up” causing an excessive drag on the wetting front.

Backpressuring of the system was another plumbing problem. If initiated correctly, the level of water in the mariotte bubbler tube will drop to the bottom fairly quickly, normally stabilization took under five minutes. If not initiated correctly, the water level in the bubbler tube will start to rise and the weight on the balance will start to increase, indicating that there is a backpressure from the cap reservoir causing water to flow back from the cap into the mariotte bottle.

Leaks in the system may affect the experiment. The soil column was mounted in the vacuum chamber using face seal fittings. These fittings not only provided a structural support for the column, but also provided the necessary hydraulic connection for the experiment. Using this combination coupling-holder also limited heat transmission via thermal bridging. Within the face seal fitting is a compression gasket, which is crushed into place to form a seal. Sometimes, these seals were reused or replaced with cheaper nylon washers. In one of the weeded runs, the head cap was leaking as a direct result of a bad fitting seal.

Packing inconsistencies can affect the soil pore geometry and thus the results of the model. In most cases, badly prepared soil samples were not used. As shown in bold type in Figure 4-2, two of the bad samples were used for experiments, the results of which were not used in further analysis.

Figure 4-2

Run	Average Bulk Density	Permeability	Maximum Percent Difference*
SC1 R1	1.41	$4.416 \times 10^{-11}$	2.95
<b>SC1 R2</b>	<b>1.54</b>	<b><math>6.455 \times 10^{-10}</math></b>	<b>115.53</b>
SC1 R3	1.41	$6.198 \times 10^{-10}$	1.38
SC1 R4	1.40	$6.565 \times 10^{-10}$	1.07
<b>SC1 R5</b>	<b>1.46</b>	<b><math>6.48 \times 10^{-10}</math></b>	<b>6.42</b>
SC1 R6	1.41	$6.764 \times 10^{-10}$	6.31
SC1 R7	1.41	$5.2186 \times 10^{-10}$	3.39
SC2 R1	1.39	$7.401 \times 10^{-10}$	-7.23
SC2 R2	1.40	$7.15 \times 10^{-10}$	0.46
SC2 R3	1.41	$6.888 \times 10^{-10}$	5.56
SC2 R4	1.41	$6.688 \times 10^{-10}$	5.44
SC3 R1	1.40	$6.17 \times 10^{-10}$	2.73
SC3 R2	1.40	$6.785 \times 10^{-10}$	1.09
SC3 R3	1.39	$6.504 \times 10^{-10}$	-1.65
AVERAGE	1.415	$6.122 \times 10^{-10}$	

\*between  $\rho_b$  of each lift and the mean  $\rho_b$

It should be noted here, however, that these two runs do say something about the effects of sample preparation. Looking at the graph of all of the runs, it can be seen that the two inconsistent runs do not follow the general slope of the rest of the runs. Since the samples were badly prepared, it is likely that care was not taken to gently and evenly pack silica powder into the column. This may cause some of the lifts to be more highly

compacted than others, resulting in an inconsistent permeability that is difficult to account for using the Kao and Hunt Model.

As a result of the weeding process, 5 runs were dropped from the data set. The following plot is of the nine “good” runs. This data set was extracted from the whole data set based on lab notes indicating problems with a particular experiment. A close examination of the plot will show that there are some data sets that conflict with all of the data, the weeding process was not based on whether or not the data agreed with the study’s presumption. Figure 4-3 shows the data sets that were dropped with the reason why the data sets were dropped.

Figure 4-3

Run Dropped	Reason
SC1 R1	Very Low Permeability
SC1 R2	Badly Packed Column, Vacuum
SC1 R5	Badly Packed Column
SC2 R2	Plumbing Problem
SC3 R2	Plumbing Problem

#### 4.2: REFINED DATA

In Figure 4-4, the symbols represent individual data points. The color code corresponds to the type of experiment; red for heated, blue for cooled, and black for room temperature. Each run is distinguished by the color code and symbol shape. The dashed lines represent the model runs at different temperatures as indicated by the legend label.

The next three plots compare data with the model predictions for the cases of lab temperature(Figure 4-5), higher temperature (Figure 4-6), and lower temperature(Figure 4-7). Data is represented by symbols and corresponding model predictions by solid lines of the same color. The legend labels represent the average temperature of the corresponding run in degrees C.

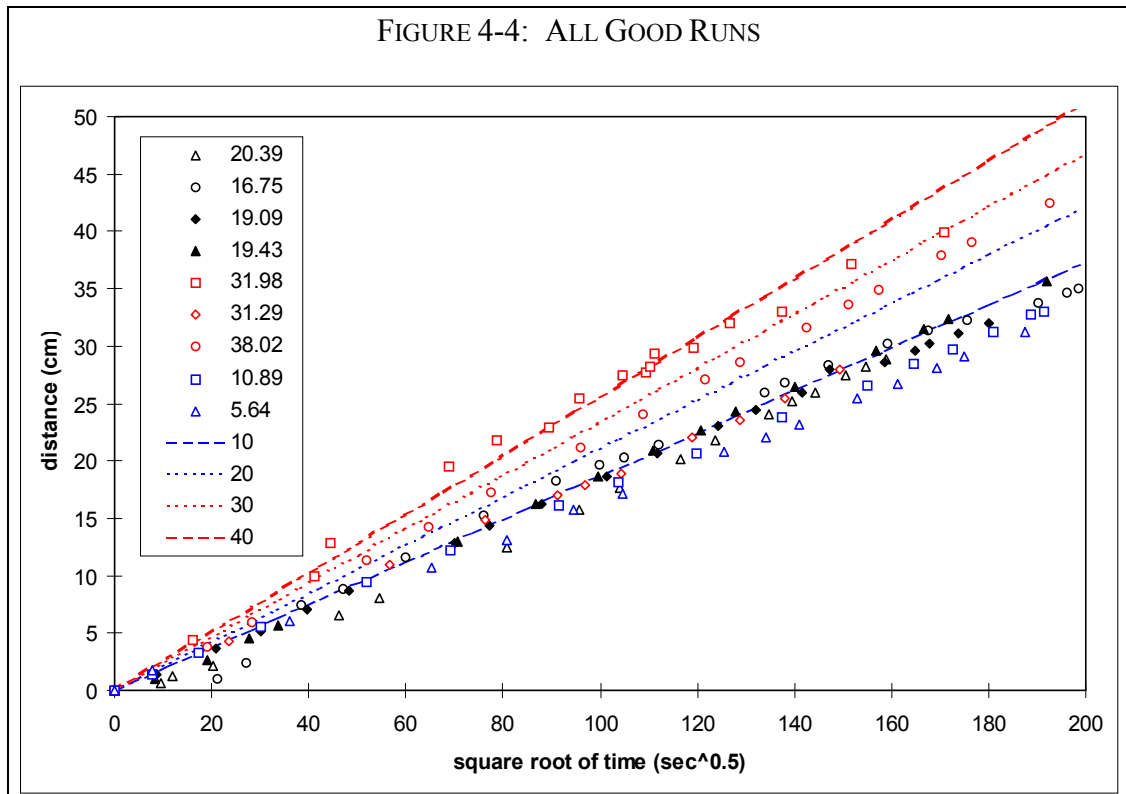


FIGURE 4-5

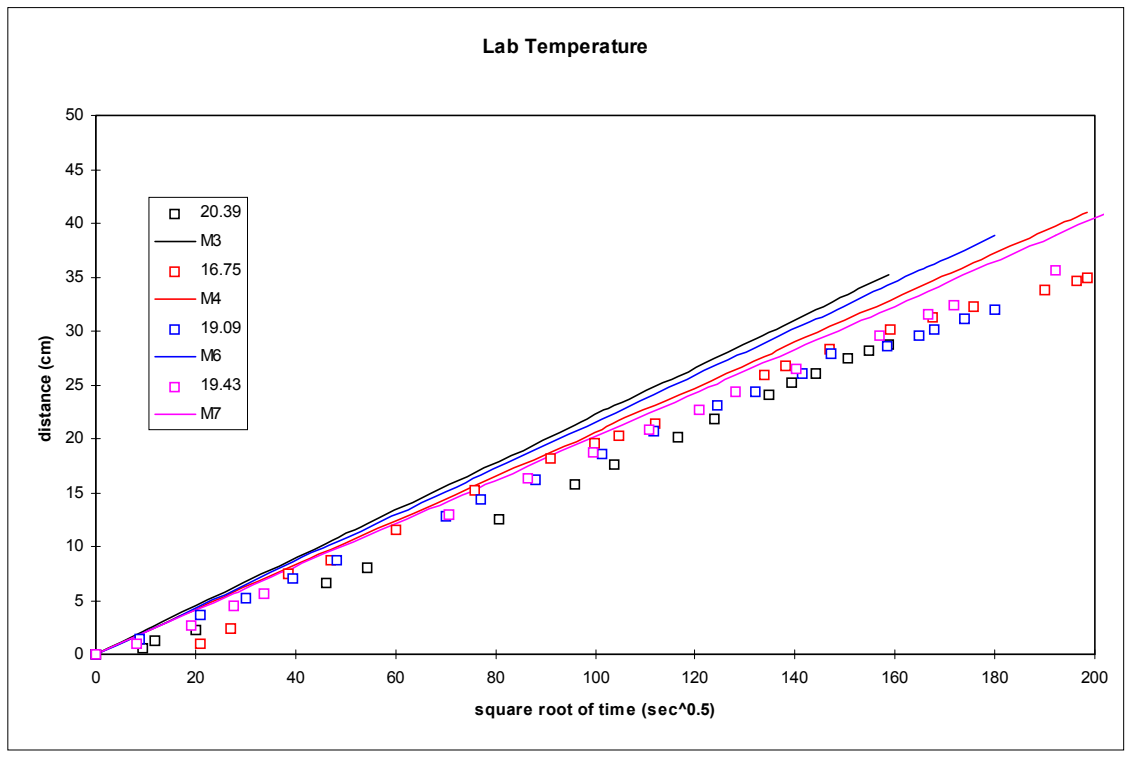


FIGURE 4-6

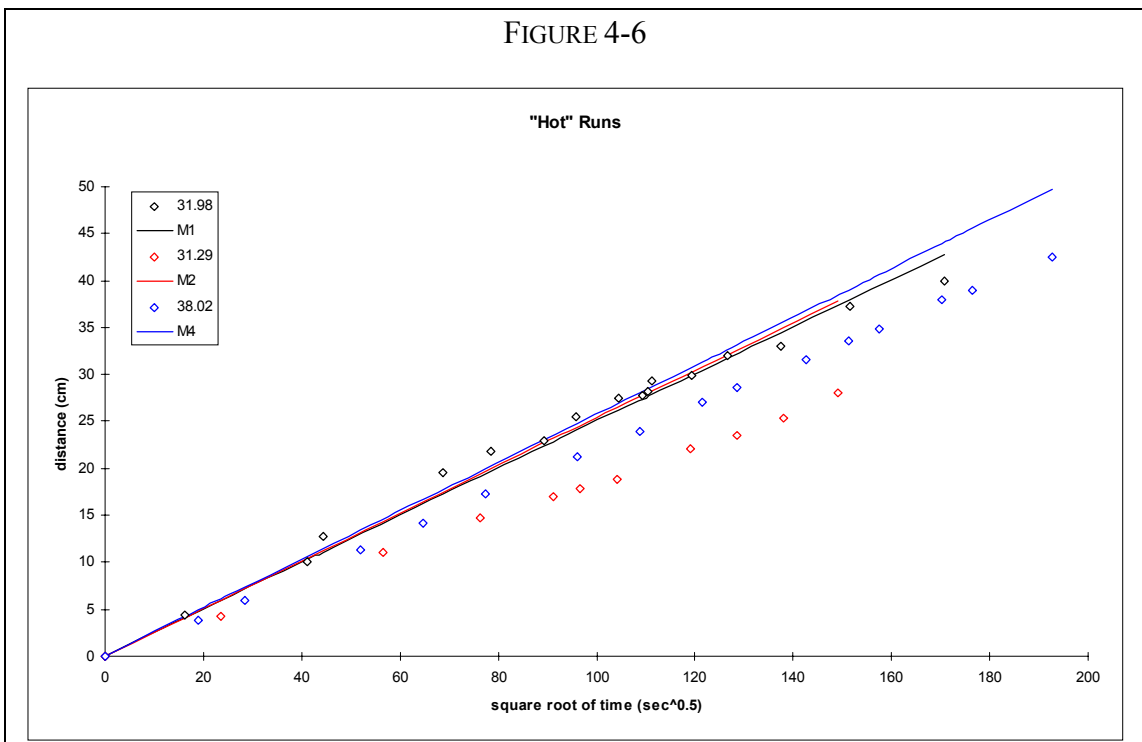


FIGURE 4-7

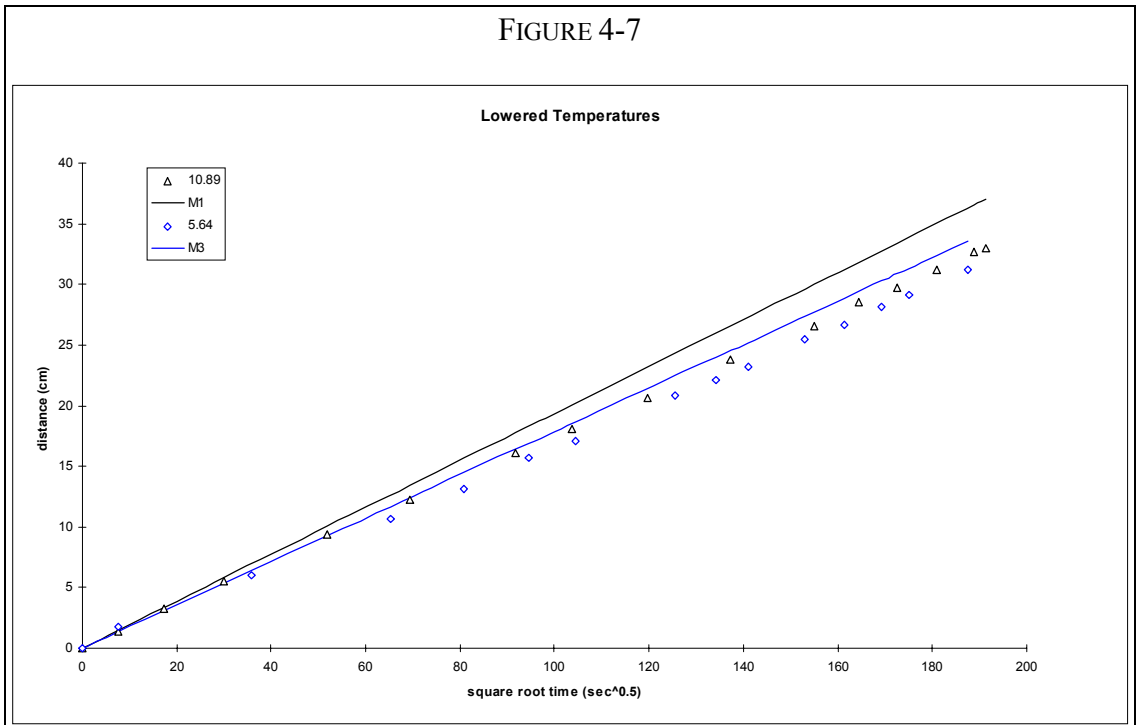
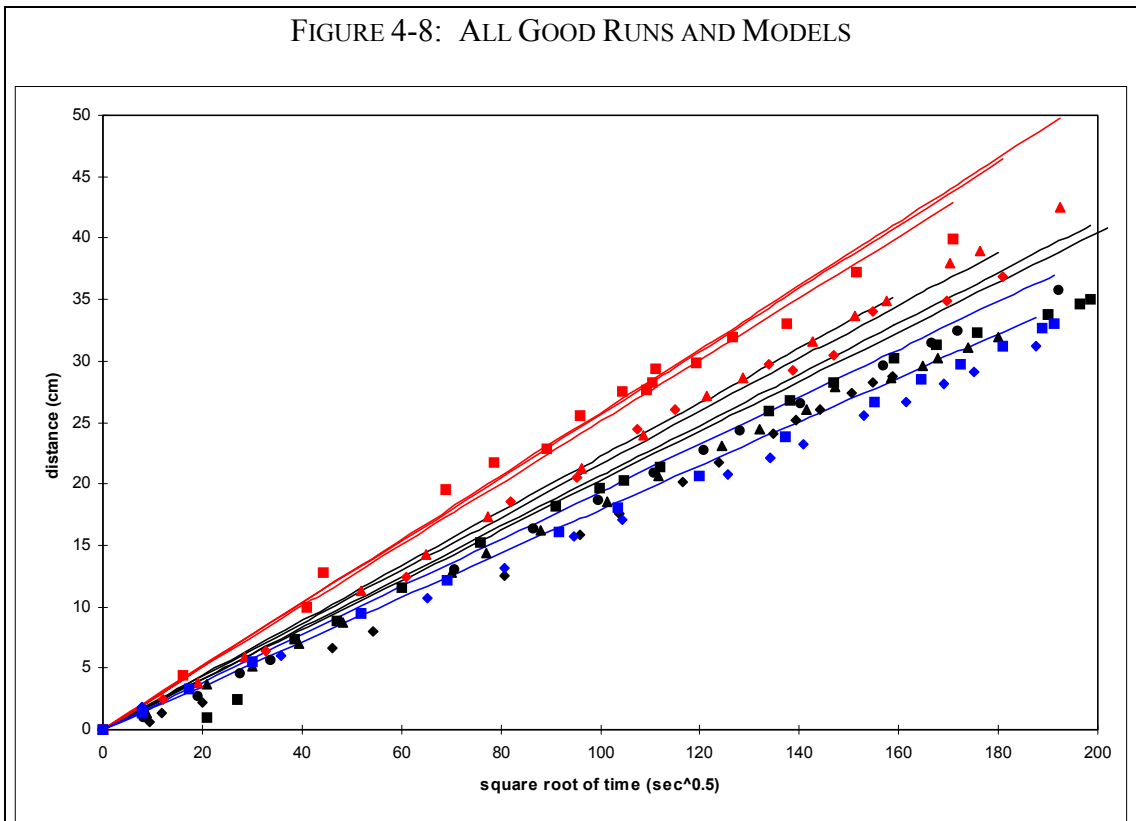


FIGURE 4-8: ALL GOOD RUNS AND MODELS





### **4.3: CONCLUSION**

It can be seen that the model predictions are in fair agreement with the experimental data, and that the error between the two is both fairly consistent and small. This implies that the hypothesis is correct, that a change in the isothermal temperatures will result in a change in the rate of infiltration.

Looking at Figure 4-8, this conclusion is further reinforced. As is expected, the model predictions for the higher temperature runs have a steeper slope than those of lower temperatures. The model predictions agree with the experimental data to within about 30 percent. The next section will discuss the data in greater detail, and look at error and the possible causes of the errors.

## **5: DISCUSSION**

This section will discuss the results of the experiments. This discussion will include:

- difference between the model and the data
- causes of experimental error
- conclusions about the data

The data, as presented in the previous chapter, implies that the wetting front tends to move faster if the temperature is increased. This tends to indicate that there is a temperature effect on the movement of the wetting front. The adapted model will be compared to the experimental data, and conclusions about the data will be drawn.

### **5.1: DIFFERENCE BETWEEN THE MODEL AND THE DATA**

For the most part, the data gathered was consistent and followed the model trend. The error associated with lab runs is similar in nature to that reported by other researchers in this general area. Figure 5-1 shows the percent difference between the model and the data. It can be seen that the data is fairly consistent in its overprediction of the speed of the wetting front, and that there is little difference in the error across experiments run at different temperatures. This shows that the simple change to the model provided a consistent and reasonably accurate adjustment of the model based on the current research standards. These errors are fairly small in comparison to errors that may be encountered in the field.

Figure 5-1: Percent Difference between Model and Data

Experiment Type	Average Percent Difference	Average Temperature
Isothermal	29.6	20.4
	14.4	16.7
	15.9	19.1
	12.7	19.4
Elevated	-3.3	32.0
	26.5	31.3
	15.2	38.0
Lowered	9.0	10.9
	5.0	5.6

Positive difference means that the model was “faster” than the data

Looking at the experimental data, it can be seen that the error associated with the different parts of the experiment are about the same. In other words, adapting the model for the appropriate values of surface tension and viscosity changed the model output enough so that the model behaves in about the same way at most temperatures within certain bounds.

## 5.2: CAUSES OF EXPERIMENTAL ERROR

The basis of using a simple model is that a large effort in formulation, modeling, and calculation, are traded for some degree of error. In some cases, the error is readily known, and is not very great. It may be worth an in-depth discussion of error in the experiment, and the model, to further validate the assumption that the simple model is reasonably accurate. In this discussion, the topics of:

- human factors
- temperature normalization of imbibed water
- non-zero pressure head

will be examined in some detail. The possible errors will be estimated by modifying the inputs to the Kao and Hunt Model.

#### **5.2.1: HUMAN FACTORS.**

The classic error in human observations of natural phenomena is reaction time. Reaction time to visual and auditory stimuli can vary; however, the normal rule-of-thumb is 0.75 sec lag in reacting to the start of an event. At two points in the experiments the accuracy of the measurement completely depend upon precise operation of a stopwatch: the timing of airflow for the permeability and the starting time of the wetting front timer, does

The average of permeameter flowrates throughout the course of the study was 45.6 sec/ml. Given the stated lag time, the expected error due to human lag is about 1.6% of flowrate. This error is damped out in the model by the fourth root taken on the permeability. Therefore, timing errors due to lag is not a significant source of error in the permeability test.

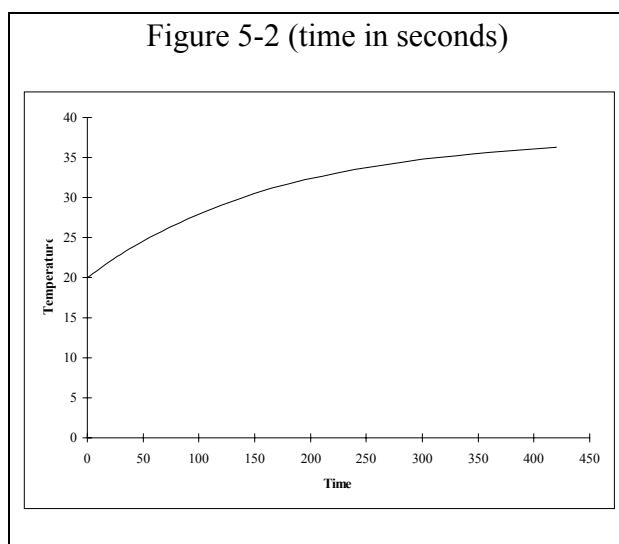
The timing of the wetting front movement also depends upon the experimenter to start the timer upon the onset of infiltration. Due to the nature of the laboratory experiment, the experimenter literally has hands full when starting a run. The effect of a delay of sixty seconds would result in an error of less than one percent.

### 5.2.2: NON-ZERO PRESSURE HEAD

An error that did seem to occur often was the backpressuring of the system. This error seems to have occurred when a smooth initialization was not achieved. During a backpressure situation, the meniscus level in the capillary vent tube of the Mariotte bottle would rise, typically to about 1.5 cm above the tube's flared bottom. The casual observer would note that an elevated pressure head at the reservoir would have the effect of driving the wetting front forward faster.

### 5.2.3: TEMPERATURE NORMALIZATION OF IMBIBED WATER

Although the temperature of the soil column was controlled for the desired range, the temperature of the imbibed fluid was held at lab temperature. Therefore, there will be a time period during which the infiltrating water will not be at the same temperature as the soil column.



The time required to heat the water at the wetting front to the temperature of the column was determined using the lumped capacity solution presented in Lienhard (1987).

$$\frac{T - T_{\infty}}{T_1 - T_{\infty}} = e^{-t/\mathbf{T}} \quad [5-1]$$

$$\text{and } \mathbf{T} = \frac{\rho c V}{\bar{h} A} \quad [5-2]$$

where:  $T$  = temperature of the body  
 $T_{\infty}$  = temperature of the fluid  
 $T_i$  = initial temperature of the body  
 $t$  = time  
 $\rho$  = body density  $\left( \frac{M}{L^3} \right)$   
 $k$  = thermal conductivity  $\left( \frac{W}{m^{\circ}C} \right)$   
 $c$  = body specific heat  $\left( \frac{J}{kg^{\circ}C} \right)$   
 $\bar{h}$  = heat transfer coefficient  $\left( \frac{W}{m^2^{\circ}C} \right)$   
 $A$  = body surface area ( $L^2$ )

The heat flux through the acrylic column was determined based on the properties and thickness of the column. The lumped solution assumes that heating and cooling occur by simple convection, where the convective fluid is the fluid pumped around the soil column during the experiments. Considering the heat flux through the column that can be provided by the water coil, for the heated case, the temperature of the water at the head of the wetting front varies according to time as shown in Figure 5-2. Since the time required for the temperature of the imbibed fluid to reach the temperature of the soil column is short compared to the duration of the experiment, the effect of the water temperature on infiltration is small.

### 5.3: DATA-MODEL ERROR

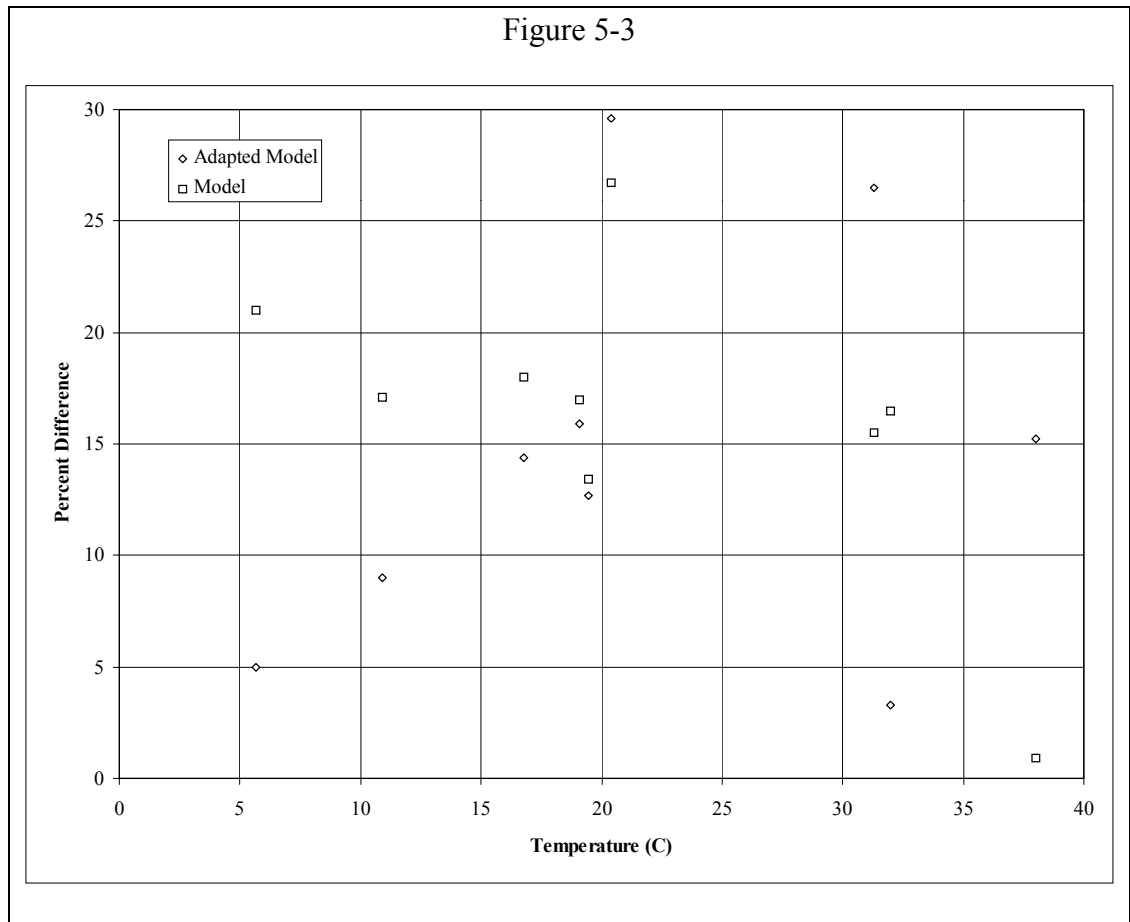
In the discussion of the difference between the model and the data, the following two views will be taken:

- temperature vs. error
- distance vs. time<sup>0.5</sup> plot slopes

These two methods of comparison were done in an attempt to show whether or not there is an obvious reason why the model is in disagreement with the data.

#### 5.3.1: *TEMPERATURE VS. ERROR*

Figure 5-3 is a scatter plot of the percent difference between the model and the average temperature. It can be clearly seen that there is not enough data and too much scatter to fit a reasonable curve to the relation between the percent difference and the temperature. This implies that there is not a clear function relating the error to the temperature; thus the error may be due to inconsistent experimental conditions rather than a clear and consistent error in the model.



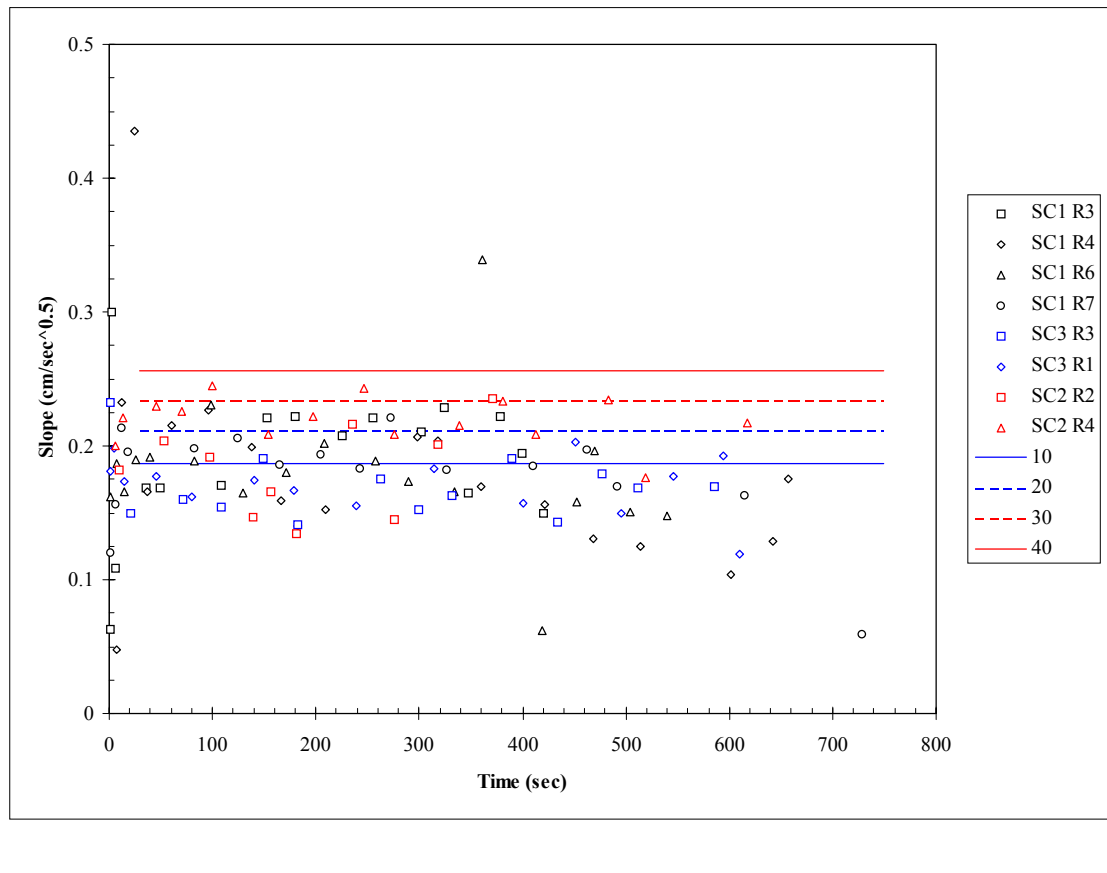
### 5.3.2: *DISTANCE VS. TIME<sup>0.5</sup> SLOPES*

The Kao and Hunt model is linear when plotted against the square root of time. If the slope of this plot is plotted against time, the model will appear as a horizontal line, and the experimental data should fall in roughly the same pattern.

Figure 5-4 is a plot of the slope of the experimental data curves. On the plot are the model predictions for the temperatures indicated in the legend. The data does not clearly reflect the stratification that is predicted by the model at different temperatures.



Figure 5-4



#### 5.4: CONCLUSION

To summarize the findings of this study, the Kao and Hunt model does produce reasonable results across a range of temperatures. It is very possible that the difference between the model and the data in this study are due to experimental error.

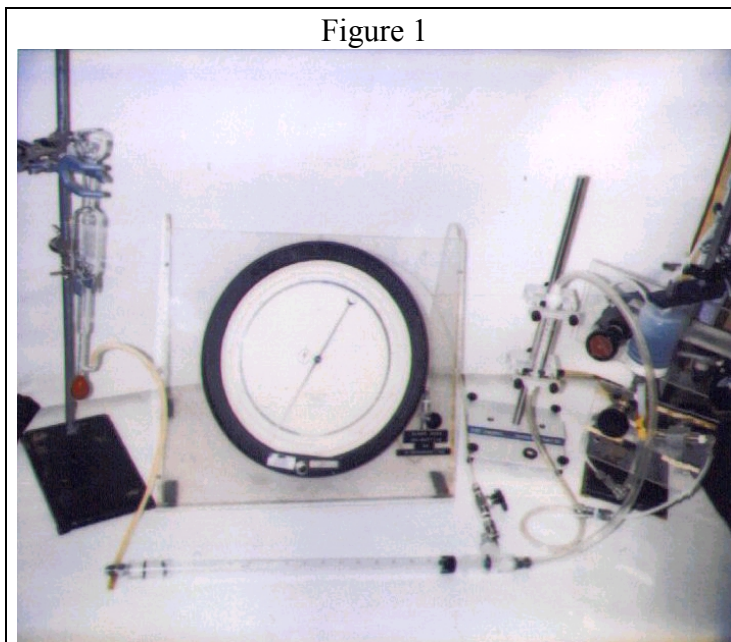
The overall effect of a change in temperature is small. This indicates that temperature variations usually encountered in the environment do not significantly affect infiltration of water. This also may not be true near heated subsurface objects there

temperature gradients are larger than those achieved in this study. This may not be true for volatile hydrocarbons, which may tend to evaporate.

Knowing the temperature of the water, the liquid effect parameters of the model can be more accurately used and tend to reduce the difference between the model and experimental data gathered.

## APPENDIX: PERMEABILITY TESTING WITH AIR

The permeability of soil can be measured using any fluid of known properties. Figure 1 shows the general arrangement of plumbing and gauges used to measure permeability using air. The path that the air sees is as follows:



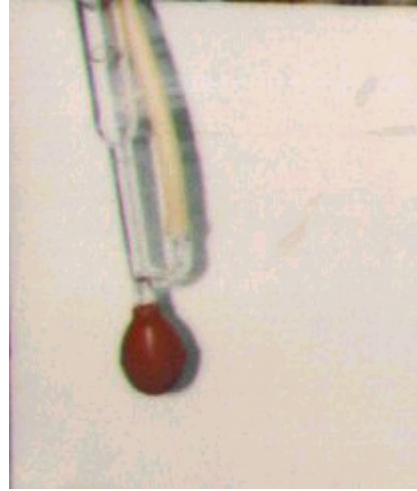
1. Air Regulation and Purification
2. High Side Flowmeter
3. Sample
4. Low Side Flowmeter
5. Atmosphere

The air regulator and purifier (far right Figure 1) is also shown in Figure 2. It consisted of two air pressure regulators in series with a carbon gas filter and a desiccator. The high side flowmeter (on stand at near right in Figure 1) was a Gilmont “Micro-Ruby” Flowmeter. Care with this flowmeter had to be taken to adjust the readings to match the calibration curve provided with the meter. The Low Side Flowmeter was a Hewlett-Packard Bubble Flowmeter. The Bubble flowmeter is also shown in Figure 3. These devices were used with a formula to determine the permeability of the soil sample. The equation used is labeled as Equation 3 on the next page.

Figure 2



Figure 3



The derivation of the equation for determining the permeability from the readings taken is as follows:

$$1. \quad Q = K \frac{\Delta h}{\Delta x} A, \text{ a form of Darcy's Law} \quad [1]$$

$$2. \quad K = \frac{k \rho g}{\mu}, \text{ definition of hydraulic conductivity} \quad [2]$$

$$3. \quad Q = \frac{k \rho g (h_1 - h_2)}{\mu \Delta x} A, \text{ substituting [2] in [1]}$$

$$4. \quad Q = \frac{k (\rho g h_1 - \rho g h_2)}{\mu \Delta x} A, \text{ algebra}$$

$$5. \quad Q = \frac{k \Delta P}{\mu \Delta x} A, \text{ definition of pressure}$$

$$6. \quad k = \frac{Q \Delta x \mu}{\Delta P A}, \text{ result} \quad [3]$$

## REFERENCES

Adamson, Arthur W. Physical Chemistry of Surfaces. 5<sup>th</sup> Edition, New York: Wiley and Sons, 1990.

Anderson, Duwayne M., Sposito, Garrison, and A. Linville. "Temperature Fluctuations at a Wetting Front: 2. The Effect of Initial Water Content of the Medium on the Magnitude of the Temperature Fluctuations." Soil Science Society Proceedings, 1963.

R.R. Bruce and A. Klute. "The Measurement of Soil Moisture Diffusivity". Soil Science Society Proceedings, 1956.

Braja M. Das Principles of Geotechnical Engineering 3<sup>rd</sup> Edition Boston: PWS Publishing Company, 1994.

C. W. Fetter Applied Hydrogeology 3<sup>rd</sup> Edition Englewood Cliffs, NJ: Prentice-Hall, 1994.

J.J. Jasper. "The Surface Tension of Pure Liquid Compounds." Journal of Physical Chemical Reference Data. Volume 1, Number 4, 1972.

Jury, W.A., Gardner, W.R., and Gardner, W.H. Soil Physics. New York: John Wiley and Sons, 1991.

C. S. Kao and J. R. Hunt. "Prediction of Wetting Front Movement During One-Dimensional Infiltration into Soils" Water Resources Research. Volume 23, Number 1, January 1996.

Lienhard, John H. A Heat Transfer Textbook. Englewood Cliffs, NJ: Prentice-Hall, 1987.

John F. McBride and Robert Horton. "An Empirical Function to Describe Measured Water Distributions From Horizontal Infiltration Experiments." Water Resources Research. Volume 21, Number 10, Pages 1539 - 1544, October 1985.

J.J. Meyer and A.W. Warrick. "Analytical Expression for Soil Water Diffusivity Derived from Horizontal Infiltration Experiments." Soil Science Society of America Journal. Volume 54, November-December 1990.

D.C. Pearce and L.W. Gold. "Observations of Ground Temperature and Heat Flow at Ottawa, Canada." Journal of Geophysical Research, Volume 64, Number 9. September 1959.

Rowell. Soil Science: Methods and Applications. United Kingdom: Longman Group, 1994.

Reid, Robert C., Prausnitz, John M., and Poling, Bruce E. Properties of Liquids and Gasses. New York: McGraw-Hill, 1987.